Wind power plants internal distribution system and grid connection
A technical and economical comparison between a 33 kV and a 66 kV

Anne Thyssen (s131448)

Kongens Lyngby 2015

Wind power plants internal distribution system and grid connection
A technical and economical comparison between a 33 kV and a 66 kV

This report was prepared by:
Anne Thyssen (s131448)

Advisors:
Mattia Marinelli, Researcher at Department of Electrical Engineering, Center for Electric Power and Energy at DTU
Claus Nygaard Rasmussen, R&D Engineer at Siemens Wind Power
Kim Høj Jensen, Power System Engineer at Siemens Wind Power

DTU Electrical Engineering
Center for Electric Power and Energy (CEE)
Technical University of Denmark
Elektrovej, Building 322
2800 Kgs. Lyngby
Denmark
Tel: +45 4525 3500
studieadministration@elektro.dtu.dk

Project period:	February 2015 - July 2015
ECTS:	30
Education:	MSc
Field:	Sustainable Energy - Electric Energy Systems
Class:	Public
Remarks:	This report is submitted as partial fulfillment of the requirements for graduation in the above education at the Technical University of Denmark.

Summary

The wind power industry today is very interested in solutions that will lower the cost of energy without compromising the technical performance of wind power plants in order to ensure that wind power remains competitive. For countries with ambitious energy targets for the future, this has become increasingly important. The present thesis challenges the traditional set up of wind power plants by investigating if using higher voltages in the collection grid results in improved technical performance and economic benefits of wind farms.

The goal of this thesis is to make a technical and economic comparison of two wind farms with a 33 kV and 66 kV collection grid. A model of both wind farms have been designed and implemented in Digsilent Powerfactory. The technical performance in terms of active power losses, reactive power capabilities, fault current and impact of using wind turbine tap changing transformers are evaluated through simulations in Powerfactory. Based on the design and technical performance of the 33 kV and the 66 kV wind farm, the economics are assessed in terms of installation cost and annual energy production.
The technical and economical evaluation are based on various conditions of the wind farms in terms of dispatched active power level and voltage set points of the wind turbines and at grid connection. The results of each wind farm are discussed and compared against each other. Furthermore, the reactive power capabilities are compared against the Danish grid code requirements.

Overall, the analysis of the technical performance and economics of both wind farms gave similar results and any differences between the wind farms were small. With this in mind, according to the comparison carried out, the benefits of using 66 kV are lower losses, slightly higher yields and lower fault currents compared to using 33 kV. However, the comparison also revealed some withdrawals of using 66 kV in terms of a small increase in the reactive power compensation needed and slightly higher installation costs. Therefore, based on the comparison carried out between the 33 kV and the 66 kV wind farm, it can not be concluded that using higher voltages in the collection grid of wind power plants will result in improved technical performance and economic benefits.

Preface

This thesis was prepared at DTU Electrical Engineering in corporation with Siemens Wind Power in the fulfilment of the requirements for acquiring an M.Sc. in Engineering in the field of Sustainable Energy with study line in Electric Energy Systems.

I would like to thank my two supervisors from Siemens Wind Power, Claus Nygaard Rasmussen and Kim Høj Jensen, for providing me with guidance and feedback whenever I needed it. I would also like to thank them and everyone else at the Siemens Wind Power office at DTU for allowing me to have a desk and a good working environment in their Siemens office for the thesis period. I would equally like to thank my DTU supervisor Mattia Marinelli for the guidance and support he has given me throughout my thesis.

Contents

Summary i

Preface iii

List of Figures vi

List of Tables vii

Glossary xi

1 Introduction 1

2 Background 5
2.1 Power Production of Wind Turbines 5
2.2 Annual Energy Production 7
2.3 Economical Assessment of Wind Power Plant 11

3 Technical Performance and Grid Connection 13
3.1 Grid Code Requirement 13
3.2 Reactive Power Capability 16
3.3 Transformer Tap Changer 20
3.4 Fault Cases 22

4 Model Design 25
4.1 Digsilent Powerfactory 25
4.2 Powerfactory Model of the 33 kV and 66 kV Wind Farm 26
4.3 66 kV Collection Grid Cables 31
4.4 Market Availability of Components 33

5 Simulations, Analysis and Results 35
5.1 Active Power Loss 36
5.2 Reactive Power Capability 41
5.3 Tap Changing Transformer Effect on P & Q 45
5.4 Fault Analysis 50
5.5 Economic Analysis 55

5.6 Comparison and Discussion 62

6 Conclusion and Future Work **69**

Bibliography **71**

Appendix **77**
A.1 ABB Datasheet Submarine Cable Systems 77
A.2 Cost Expression Parameters 79

List of Figures

2.1 Rotor area and hub height of wind turbines since 1980 6
2.2 Power curve Siemens wind turbine 3.6-120. 6
2.3 Weibull distribution at Hvide Sande and Horns Rev 9
2.4 Annual energy production when losses are taken into account. . . 10
2.5 Levelised cost of onshore and offshore wind energy over time . . 12

3.1 Energinet.dk's reactive power requirement for wind power plants 15
3.2 Energinet.dk's voltage and reactive power requirements 15
3.3 Reactive power capability of wind turbine 19
3.4 Basic example of an De-Energized tap changing transformer . . . 21
3.5 Example of an On Load tap changing transformer 21

4.1 Layout of wind farm 27
4.2 Layout of wind turbine AA01 28

5.1 Energy loss of the wind farms at Horns Rev and Hvide Sande. . . 37
5.2 Efficiency for the 33 kV wind farm and 66 kV wind farm. 38
5.3 Distribution of energy losses in the 33 kV and the 66 kV wind farm 38
5.4 Energy loss comparison between the wind farms 39
5.5 Reactive power capability at grid voltage of 1 pu. 41
5.6 Reactive power capability at grid voltage of 0.9 pu. 42
5.7 Reactive power capability at grid voltage of 1.06 pu. 42
5.8 Active power losses for all taps at WT trf in 33 kV wind farm . . 46
5.9 Active power losses for all taps at WT trf in 66 kV wind farm . . 46
5.10 Reactive power capabilities at tap position -1 for Vgrid = 0.9 pu. 49
5.11 Fault current for a three phase short circuit fault. 50
5.12 Impedance for fault location at WT AA01 transformer 52
5.13 Fault current at single line to ground fault. 54

A.1 Current rating for three-core submarine ABB cables 77
A.2 Technical data for ABB 66 kV three-core submarine cables 78

List of Tables

2.1 Weibull distribution parameters and mean wind speed 8

3.1 Reactive power production and absorption of components 17
3.2 Four common short circuit faults 23

4.1 Main similarities/differences between the two Powerfactory models. 26
4.2 General information about the 33 kV and the 66 kV wind farm. . 28
4.3 The wind turbine transformers modelled in Powerfactory 29
4.4 The substation transformers modelled in Powerfactory. 30
4.5 Specification of cables used in the 33 kV wind farm 30
4.6 Specification of collection grid cables in the 66 kV wind farm . . 32

5.1 Costs of the 33 kV wind farm. 59
5.2 Costs of the 66 kV wind farm. 59
5.3 AEP of the 33 kV wind farm and the 66 kV wind farm. 60
5.4 Summary and comparison of results between the two wind farms. 62

A.1 Cost expression parameters 79

Glossary

List of Symbols

$A_{(cable)}$	Cross section area of cable [m^2]
$A_{(rotor)}$	Rotor area [m^2]
$A_{(weibull)}$	Weibull scale parameter [m/s]
C	Capacitance [F]
C_{cable}	Cost of cables [€]
C_{losses}	Cost of energy losses [€]
C_{SG}	Cost of switchgear [€]
$C_{shunt\ reactor}$	Cost of shunt reactor [€]
C_{trf}	Cost of transformer [€]
C_p	Aerodynamic efficiency [%]
E_{loss}	Total energy loss wind farm [Wh]
E_{total}	Total energy output wind farm [Wh]
f	Frequency distribution [%]
I	Current [A]
$I^f_{a/b/c}$	Phase a, b or c fault current[A]
k	Weibull form parameter
l	Length of cable [km]
L	Inductance [H]
$n_{(no.\,of\,WT)}$	Number of wind turbines in a wind farm
$N_1\ N_2$	Number of turns primary and secondary winding, respectively
P	Power [W]
$P_{CF\,average}$	Average power of wind farm using the capacity factor [W]
P_{nom}	Nominal power of a wind power plant [W]
P^{WT}_{nom}	Nominal power of a wind turbine [W]
P^{out}_u	Power output at PCC at wind speed u [W]
$P^{WT\,out}_u$	Active power of a wind turbine at wind speed u [W]
Q	Reactive Power [VAr]
R	Resistance [Ω]

S	Apparant Power [VA]
SIL	Surge Impedance Load [V/Ω]
Δt	Time period [h]
T	Temperature [^oC]
U	Wind Speed [m/s]
V	Voltage [V]
V_1 V_2	Primary and secondary voltage, respectively [V]
$V^f_{a/b/c}$	Phase a, b or c fault voltage [V]
X	Reactance [Ω]
$Z^{'}$	Impedance referred to the primary side of transformer [Ω]
Z_c	Source impedance [Ω]
Z_f	Fault impedance [Ω]

α_0	Temperature coefficient
α_{ICC}	Estimated increase/decrease in ICC for 66 kV compared to 33 kV [%]
α_t	Turns ratio
β	Current angle [degrees or radians]
β_{AEP}	Estimated increase/decrease in AEP for 66 kV compared to 33 kV [%]
δ	Voltage angle [degrees or radians]
γ_p	Proximity effect factor
γ_s	Skin effect factor
λ	Tip speed ratio [rad]
ϕ	Phase angle between voltage and current [degrees or radians]
ρ_{air}	Air density [kg/m^2]
$\rho_{conductor}$	Resistivity of conductor material [Ω m]
σ_u	Probability of wind speed [%]
θ	Pitch angle [deg]

Abbreviations

AC	Alternating Current
AEP	Annual Energy Production
AOE	Annual Expenses
CF	Capacity Factor
DC	Direct Current
DETC	De-Energized Tap Changers
ENTSO-E	European Network and Transmission System Operators for Electricity
EPR	Ethylene Propylene Rubber
FCR	Fixed Charge Rate
HV	High Voltage
ICC	Installed Capital Cost
LCOE	Levelised Cost of Energy
LV	Low Voltage
Nom	Nominal
OLTC	On Load Tap Changers
SC	Short Circuit
SG	Switchgear
PCC	Point of Common Coupling
PF	Power Factor
PV	Active Power & Voltage magnitude (control)
Trf	Transformer
WF	Wind Farm
WPP	Wind Power Plant
WT	Wind Turbine
XLPE	Cross-Linked Polyethylene

Chapter 1

Introduction

The utilisation of wind energy is known to have been around for more than 3000 years when it was first used for mechanical power purposes such as pumping water or grinding grains. In the late 19th century the first developments of an electrical generating wind turbine has been documented in different parts of the world. For example, in 1891, the Dane Poul La Cour developed one of the first electrical generating wind turbines and by 1918 3% of the electricity demand in Denmark was supplied by wind energy [18].
In the last decades wind power has gained increasing importance throughout the world due to its environmental benefits and the energy security it provides. These benefits are equally liable for all renewable energy sources, however, wind power has become one of the dominating technologies within the renewable energy sector due to its cost competitiveness [43] [74].

The growing wind industry within Europe contributes to reach EU's energy target of having 20% of the EU's energy consumption covered by renewable energy sources by 2020 and 27% by 2030 [31] [29] [30]. Some countries have extended the energy targets set by EU. Denmark has, for example, the ambitious goal of having approximately 50% of the electricity consumption covered by wind energy by 2020 and reaching 100% renewable energy in the energy and transport sector by 2050 [20].

As a result of EU and country specific energy targets, the wind industry has experienced a positive growth in recent years both concerning onshore and, particularly, offshore developments. In past decades the majority of wind power installations were onshore and today in Europe alone there is 129 GW of onshore installed wind energy capacity [32]. Offshore wind energy was first seen in Denmark with the 5 MW offshore wind power plant (Vindeby) installed in 1991 However, since the commitment to the EU's energy targets, the offshore wind

industry has increased significantly since Vindeby was erected. As of 2014, the size of an average offshore wind farm is 368 MW and the total installed offshore wind capacity in Europe is 8 GW [32]. It is expected that the offshore wind industry will increase significantly in the future with an estimated installation of 40 GW offshore power by 2020 and 150 GW by 2030 in Europe [23].
As the wind industry grows so does the size of wind turbines and the size of wind power plants. At the same time, there is a tendency for offshore wind farms to be placed further away from shore. Despite these developments within particularly the offshore wind industry, offshore wind farms today are still designed and built following the traditional set up of wind farms. The standard offshore wind farm uses 33 kV in the internal electrical grid which is then stepped up to a voltage between 110 kV to 220 kV at the offshore substation before the power is transported to land. The increasing size of turbines, wind farms and distance to shore combined with less local or European incentives are driving up the cost of offshore wind. In order for offshore wind energy to remain cost competitive, drivers to bring down the cost are highly sought for.

In addition to this, power systems that experience the increasing share of wind energy are faced with some challenges due to the fluctuating nature of wind energy. The main aims of transmission system operators are to maintain the power balance between generators and consumers at all times and to keep the voltage within acceptable limits. In order to obtain a secure and efficient operation of the power system specific grid connection requirements for wind farms have been developed in recent years [18].

Significantly amount of research is therefore focusing on solutions to lower the cost of energy for offshore wind farms without compromising the grid code requirements set by power system authorities. Based on this, current research documented in literature challenges the traditional standard wind farm, investigating whether this is the most cost effective solution for future offshore wind power plants.
A new topic under research explores the option of using higher voltages in the internal grid of wind farms compared to the traditional set up using 33 kV. In the literature review conducted for this thesis, a limited amount of published work on this topic have been found. Similar initial conclusions are drawn by the literature reviewed. According to [40], [49],[65], [68] and [15] the results of using higher voltages in the collection grid will potential lead to cost reductions. The largest cost reduction is caused by the possibility of removing the offshore substation transformer in wind farms of higher voltages [49] [15] [40]. Other benefits include lower losses and lower short circuit levels [49] [68].

This project dives deeper into the research topic of using higher voltages in the collection grid. The initial hypothesis is that using higher voltages will lead to lower losses and lower fault current but also higher cost of components. The

purpose of the project is therefore to investigate the influence that the choice of voltage level in internal grids for wind power plants has on their technical performance and economy. The investigation is based on a comparison between a generic standardised wind farm using 33 kV voltage in the internal grid and a wind farm using 66 kV in its internal grid. The investigation includes an analysis using a simulation model of two wind parks implemented in the power system simulation software DigSilent Powerfactory.

The technical performance of the 33 kV and the 66 kV wind farm is investigated in terms of the electrical active power losses within the wind farms and the reactive power capabilities of the wind farms. When evaluating and comparing the results of the reactive power capabilities, focus is kept upon how the results fulfil the Danish grid code requirements. The losses and reactive power capabilities are investigated for various conditions of the wind farms, for example for different exported power levels and different voltage set points at grid connection. The influence of using tap changing wind turbine transformers is also analysed regarding the losses and reactive power capabilities. Furthermore, the technical performance of the two wind farms includes an investigation of the fault current in different fault cases.

The outputs of the technical performance lay the ground of the economic analysis. The economic aspects are studied by comparing the technical requirements of the equipment in the two wind farms and summarizing the installation costs of relevant components. The cost of active power losses in the two cases is also evaluated. The economic aspects are further discussed in terms of cost of energy of each wind farm estimated relatively to each other. The estimation of cost of energy is based on the results of the installation cost and the annual energy production of the 33 kV and the 66 kV wind farm.

The report has been built up as follows: In chapter 2 of this thesis the theoretical background of wind power is introduced in terms of power production and annual energy production including background knowledge concerning the economics of wind farms. Chapter 3 provides the theoretical background of the technical performance parameters that the technical comparison between the 33 kV and the 66 kV wind farm are based upon. Chapter 4 presents the model design of the two wind farms implemented in the simulation tool Powerfactory and a brief discussion of the market availability of components are also included here. Chapter 5 presents the most important results of the simulations carried out and associated analysis and discussion of the technical performance and the economics of the 33 kV and the 66 kV wind farm is included. Furthermore, chapter 5 includes an overall comparison between the two cases and the results are put into perspective. Finally, in chapter 6 the main conclusion of the project is summarised and ideas to extend the research are proposed.

Chapter 2

Background

This chapter gives an introduction into wind power. The power production of wind turbines is introduced and the aerodynamic power of wind turbines is presented as well as a wind turbines' power curve is illustrated. The Weibull distribution in relation to wind power has been elaborated upon and, as example, the Weibull distribution at two sites, Horns Rev and Hvide Sande, is evaluated. In addition to this, the annual energy production of wind farms is further discussed and associated with this the capacity factor of Horns Rev and Hvide Sande is estimated. Finally, the chapter includes a brief introduction into the economics of wind farms.

2.1 Power Production of Wind Turbines

The aerodynamic power of a wind turbine (WT) can be expressed by equation 2.1. It reflects how much power is possible to extract from the wind. The aerodynamic power is a function of the air density ρ, the wind turbine's rotor area A, the wind speed U and the aerodynamic efficiency C_p [45].
The aerodynamic efficiency can theoretical not exceed Betz limit of 59%. It can be expressed as a function $C_p(\lambda,\ \theta)$, hence, depends on the pitch angle θ and the tip speed ratio λ [45]. Therefore, if the wind turbine enables it, the aerodynamic efficiency can be controlled by adjusting the pitch angle and the rotor speed. Today, the most common control option for wind turbines is pitch control with other options being stall control and active stall control [18].

$$P = \frac{1}{2}\ \rho\ A\ U^3\ C_p \tag{2.1}$$

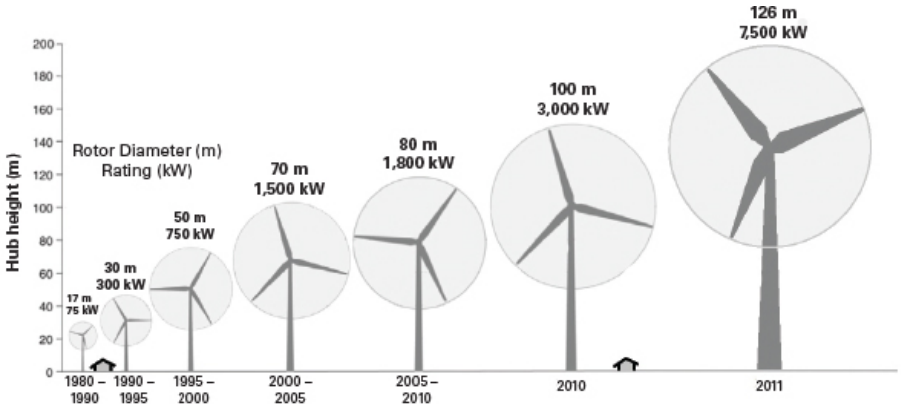

Figure 2.1: Rotor area and hub height of wind turbines since 1980 [63].

The power production of wind turbines will increase if the rotor area increases and/or if the wind turbine is put in an area with higher wind speeds. The increase of rotor area is clearly seen in the production of wind turbines in the past decades, as illustrated in figure 2.1.

The actual power output of a wind turbine is limited by physical restrictions and is best illustrated by a power curve. The power curve of a wind turbine shows the electrical power output of the wind turbine at specific wind speeds. The power curve of Siemens wind turbine 3.6-120 is shown in figure 2.2 created with data from [10]. The Siemens 3.6 MW wind turbine is used in the models of the two wind farms (WF) for the evaluation of the technical performance.

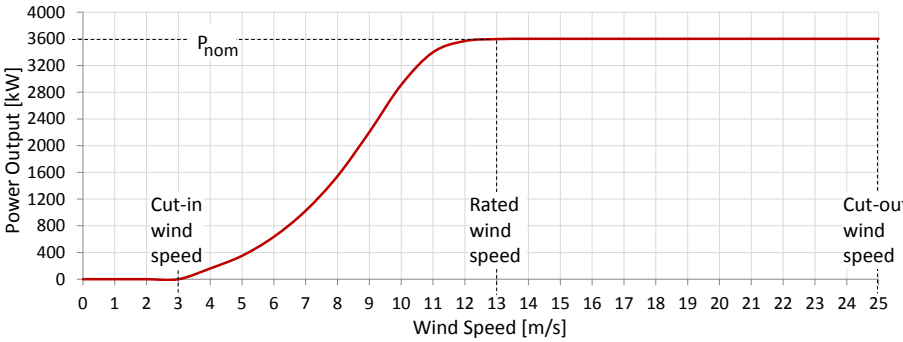

Figure 2.2: Power curve Siemens wind turbine 3.6-120.

The operating range of the wind turbine is defined by the cut-in and cut-out wind speed. The cut-in wind speed, shown in the power curve, is the sufficient wind speed for the generator to operate and produce electric energy. When the cut-out wind speed is reached the power production of the wind turbine is cut off. The rated wind speed is the wind speed at which the rated nominal power of the wind turbine is reached.
In order to avoid mechanical stresses, which potential could destroy the wind turbine, the power is kept at nominal output once the rated wind speed is reached and the production of the turbine is stopped when the cut-out wind speed is reached. Hence, this zone between the rated and the cut-out wind speed is called the limitation zone and the wind turbine is designed and controlled to limit its output power within the limitation zone. The limitation of the output power within the limitation zone is achieved by reducing the efficiency of the energy conversion of the wind's kinetic energy into mechanical energy. The zone between the cut-in wind speed and the rated wind speed is the optimisation zone where the wind turbine is designed and controlled to optimise the aerodynamic efficiency.

The output power of the wind turbine at each wind speed in figure [10] has been used to calculate the expected power production of a wind turbine at a specific site with a known Weibull distribution. This is elaborated upon in section 2.2.

2.2 Annual Energy Production

Weibull Distribution

The annual energy production (AEP) of wind turbines is highly dependant on the wind speeds of the area that the wind turbines are erected, as seen by equation 2.1 and figure 2.2. In order to estimate the annual energy production of a wind farm it is therefore necessary to have an estimation of the wind speeds at its location.

The Weibull distribution can be used as an approximation of the wind speed distribution at specific sites. The Weibull distribution will show a graph where the frequency of the wind speed at a specific site is plotted as a function of the wind speed. Hence, it shows the frequency distribution of wind speeds and mathematically it can be described as a function depending on two site specific parameters. The expression of the Weibull distribution is shown in equation 2.2 [44].

$$f(u) = \frac{k}{A} * \left(\frac{u}{A}\right)^{k-1} exp\left(-\left(\frac{u}{A}\right)^{k}\right) \tag{2.2}$$

Here $f(u)$ is the frequency distribution of the wind speed where u is the wind speed. The two parameters A and k are specific for the site investigated and is generally obtained with measurement of wind speed using anemometer on the site. A is the Weibull scale parameter and is measured in m/s. It is proportional to the mean wind speed of the site and provides the characteristics of the wind speed distribution. k is called the Weibull form parameter and is unit independent, generally a number between 1 and 3. It defines the shape of the Weibull distribution where a high value of k characterises sites with more constant wind speeds while a low value of k characterises sites with high wind speed fluctuations [57].

Through literature research, the site specific parameters A and k have been found for two sites in Denmark and the Weibull distribution for these two sites have been chosen to investigate further. The first site is at the location of Horns Rev located in the North Sea. The other site is Hvide Sande, very close to the North Sea, on the west coast of Jutland.

The Weibull shape and scale factor for the two sites are taken from [46] where the wind is measured for a period from 1999 to 2002 on the two sites. The measurements at Horns Rev are taken at a height of 62 m while at Hvide Sande the height for the anemometer is 27.5 m.The results are summarised in table 2.1.

Table 2.1: Weibull distribution parameters A and k and mean wind speed at Horns Rev and Hvide Sande [46].

	A [m/s]	k	Mean wind speed u_{mean}[m/s]
Hvide Sande	7.81	2.23	6.9
Horns Rev	10.71	2.33	9.5

Equation 2.2 is used to find the frequency occurrence of different wind speeds using A and k for each site. Hence, the Weibull distribution for Hvide Sande and Horns Rev is illustrated in figure 2.3.

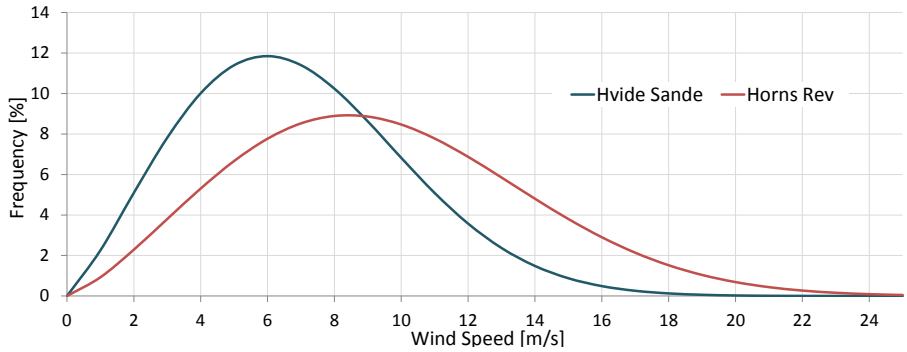

Figure 2.3: Weibull distribution of wind speeds at Hvide Sande and Horns Rev.

Annual Energy Production

The annual energy production of a wind farm using the Siemens 3.6 MW wind turbines erected at Horns Rev or Hvide Sande can be estimated using the power curve in figure 2.2 and the Weibull distribution in figure 2.3. This is expressed by equation 2.3 where σ_u is the probability from the Weibull distribution that the wind has a speed of wind speed u and $P_u^{WT\,out}$ is the power output of a wind turbine from the power curve at wind speed u. The range of the wind speed is set from 3 m/s to 25 m/s to represent the cut-in and cut-out wind speed of the Siemens 3.6 MW turbines, respectively. $n_{no.ofWT}$ is the number of wind turbines in the wind farm and Δt is the time period and for 1 year = 8760h. Expression 2.3 does not take any kind of losses into account and it assumes that the Weibull distribution obtained for Hvide Sande and Horns Rev is a close representative of the distribution of wind speeds within one year.

$$AEP_{virtual} = \sum_{u=3-25\mathrm{m/s}} \left(\sigma_u \; P_u^{WT\,out}\right) * n_{(no.\,of\,WT)} * \Delta t \tag{2.3}$$

The losses neglected in the calculations of AEP in equation 2.3 are best illustrated by a drawing. Figure 2.4 shows that the AEP also depends on wake losses, losses in the internal grid of the wind farm and potential outages of one or more wind turbines within the time period considered.
In this project, it is looked into whether the electrical losses are different and how it affects the AEP when using higher voltages in the internal grid. The loss analysis is presented in section 5.1. Other assessments carried out in this project concerning the technical performance of wind farms are introduced in chapter 3.

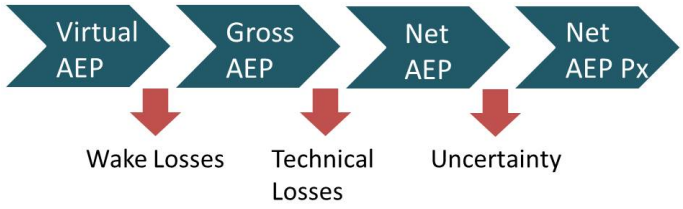

Figure 2.4: Annual energy production when losses are taken into account.

Capacity Factor

The annual energy production is also used to calculate the capacity factor (CF). The capacity factor can be used to assess how efficient a site is. It is defined as the produced power in relation to the nominal power of the wind farm as expressed by equation 2.4. Here Δt_{year} is equal to the hours in a year (8760h) and P_{nom} is the nominal power of the wind farm [18].

$$Capacity\ Factor\ CF\ [\%] = \frac{Net\ Annual\ Production[\text{MWh}]}{\Delta t_{year} * P_{nom}[\text{MW}]} \tag{2.4}$$

The capacity factor for Horns Rev and Hvide Sande has been estimated using the simplified expression for AEP in equation 2.3. Hence, the capacity factor of the two sites is estimated according to equation 2.5, where P_{nom}^{WT} is the nominal power of each wind turbine.

$$\begin{aligned} CF_{estimated}\ [\%] &= \frac{\sum_{u=3-25\text{m/s}} \left(\sigma_u * P_u^{WT\,out}\right)\ n_{(no.\ of\ WT)} * \Delta t}{P_{nom}^{WT} * n_{(no.\,of\,WT)} * \Delta t} \\ &= \frac{\sum_{u=3-25\text{m/s}} \left(\sigma_u * P_u^{WT\,out}\right)}{P_{nom}^{WT}} \end{aligned} \tag{2.5}$$

Using equation 2.5, the capacity factor for Horns Rev is 58.7% and for Hvide Sande it is 36.1%. The difference between Horns Rev and Hvide Sande is caused by how the wind speed is distributed in relation to the power curve of the wind turbines. As the Weibull distribution for Hvide Sande peaks at a lower wind speed around 6 m/s and has a more narrow curve compared to Horns Rev, where the occurrence of higher wind speeds is more frequent, the capacity factor at Hvide Sande is much lower compared to the CF of Horns Rev.

This is also a reason why it is important to consider which wind turbines to erect on a site, as a turbine with a power curve more favourable to lower wind speeds would improve the capacity factor for Hvide Sande significantly.

Note that, calculating the capacity factor in this way, no losses are taken into account and the estimated energy production relates to the virtual AEP. Hence, the energy production used to calculate the capacity factor is too high resulting in a higher capacity factor compared to the capacity factor of the sites if a wind farm, as the one in consideration, where erected at Horn Rev and at Hvide Sande. This also explains why the capacity factor at particularly Horns Rev is higher than the capacity factor obtained from studies of existing wind farms. According to [22] the average capacity factor of all offshore wind farms in Denmark, within a 12 months period from March 2014 - March 2015, is 42.9%, where Horns Rev II came out with the highest capacity factor of all offshore wind farms in Denmark with $CF = 48.4\%$.
Despite this, it has been decided for this project that the calculated capacity factor still can be used as it is only used to define a specific set point for the dispatched power. The average output power of a wind turbine related to the capacity factor for Horns Rev is 58.6% * 3600 kW = 2112 kW and for Hvide Sande it is 1301 kW.

2.3 Economical Assessment of Wind Power Plant

The levelised cost of energy (LCOE) is often used as a measure of the cost of generating power from a particular unit which is then comparable between different generation units. It is calculated using the total lifetime cost of generation and the total net annual energy production of the same unit. The average LCOE of onshore wind farms is very competitive to non renewable technologies, however, LCOE of offshore wind is significantly higher compared to conventional generating units [19]. The development of LCOE for onshore and offshore wind in recent years is illustrated in figure 2.5. Since 2009 to 2013 LCOE for onshore wind has decreased with 18% but due to the harsh construction environment of offshore wind, as a results of projects developed further from shore, the cost of offshore wind has increased from 2009 to 2013 [8]. However, it is expected that LCOE of offshore wind will become highly competitive compared to other energy sources by 2023 due to the industry's continues effort of driving the installation and operation and maintenance cost down [14].

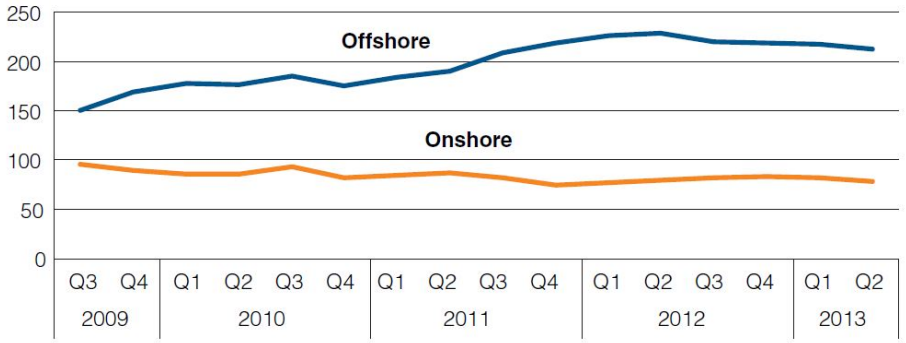

Figure 2.5: Levelised cost of onshore and offshore wind energy over time [USD/MWh] [8].

According to [67] LCOE can be calculated as expressed in equation 2.6. It is seen that LCOE depends on four parameters: The installed capital cost *ICC*, the annual expenses AOE, the annual energy production AEP and the fixed charge rate FCR. FCR represents the costs of financing a project while ICC, AEP and AOE are design system specifics.

$$LCOE = \frac{(ICC * FCR) + AEO}{AEP_{net}} \tag{2.6}$$

From the equation of LCOE in 2.6 it is seen that LCOE of a project can be reduced by decreasing the installation cost and the operation expenses or by increasing the annual energy production.

The design and technical performance of the 33 kV and 66 kV wind farm, investigated in this thesis, will provide data for the electrical losses within the wind farms and technical requirements of the components in the wind farms. As the AEP of a wind farm can be increased by decreasing the electrical losses in the internal grid, potential differences in AEP for the two wind farms investigated can be estimated. The installation cost depends on the technical requirements of the equipment, hence, differences in ICC of the two wind farms is equally investigated. The associated economic calculations and discussion of the effects that AEP and ICC for the two wind farms have on LCOE is provided in section 5.5.

Chapter 3

Technical Performance and Grid Connection

Chapter 3 introduces the theoretical background related to the technical evaluation of the two wind farms. This includes an introduction of reactive power and reactive power capabilities of wind farms, where the reactive power capability of the wind turbines used in the model is presented. In relation to the reactive power capabilities, the grid code requirements are discussed and the Danish reactive power requirements for wind power plants from Energinet.dk are presented. The theoretical background of transformers and tap changing transformers used in wind power plants is also elaborated upon in this chapter. Finally, an introduction into fault analysis is included and an overview of the four most common faults is presented.

3.1 Grid Code Requirement

The main aim for the power system is to cover the demand of all electricity consumers and doing so while delivering the electricity whenever the consumers need it, hence, a secure and stable operation of the grid has the highest priority [48]. In order to accomplish this, a set of rules and regulations are formed and captured in what is called grid codes. Grid codes describe the technical specifications and requirements of the components in the power system. Grid code requirements are defined by network authorities and have been used for many years in the operation of the power system. Due to the increase of wind power in the power system in some countries, a need for specific grid codes concerning wind power plants (WPP) has occurred. The regulations concerning wind power plants ensure that the power system remains balanced and the

voltage level remains within limits at all time, despite the fluctuating nature of wind [48].

The European Network and Transmission System Operators for Electricity (ENTSO-E) consists of 41 transmission system operators from 34 European countries. Since 2009 it has had legal status and as a result a set of grid code requirements for the transmission system operator (TSO) have been developed [7]. The requirements are in place to promote and support [5]:

- The increasing integration of renewable energy into the power market, as a result of the EU energy targets.
- The cooperation and cross border trade between countries and in adjacent to this supporting the internal energy market.
- The operation of a secure and stable power system.

As Denmark is part of the Nordic power system the ENTSO-E requirements must be followed. The ENTSO-E requirements are less detailed compared to the local network requirements issued by the TSO. In Denmark Energinet.dk has the responsibility of operating the grid and the grid code requirements must at least fulfil the requirements set by ENTSO-E.

For the scope of this thesis, requirements concerning reactive power capability of wind power plants have be focused upon. Reactive power Q is an important feature of voltage stability. The control of voltage levels is accomplished through absorption and generation of reactive power. In general terms, absorbing reactive power decreases the voltage and generating reactive power increases the voltage level.

According to ENTSO-E every TSO shall define a U-Q/Pmax-profile and P-Q/Pmax-profile for which power plants must be capable of moving their operating point within a defined area. The defined U-Q/Pmax profile should also emphasise that reactive power production at high voltage (HV) and reactive power consumption at low voltages (LV) might be unnecessary. The reactive power capabilities for wind power plants shall be specified at connection point, hence, the WPP can use different control modes in order to meet the requirements as well as incorporating any compensation at connection point [6].

Due to the significant amount of wind power integrated into the Danish power system, Denmark has established a set of grid codes which provide the minimum set of requirements that a wind power plant must fulfil when connected to the Danish grid. From this, the defined reactive power requirements for wind power plants larger than 25 MW are shown in figure 3.1 and 3.2.

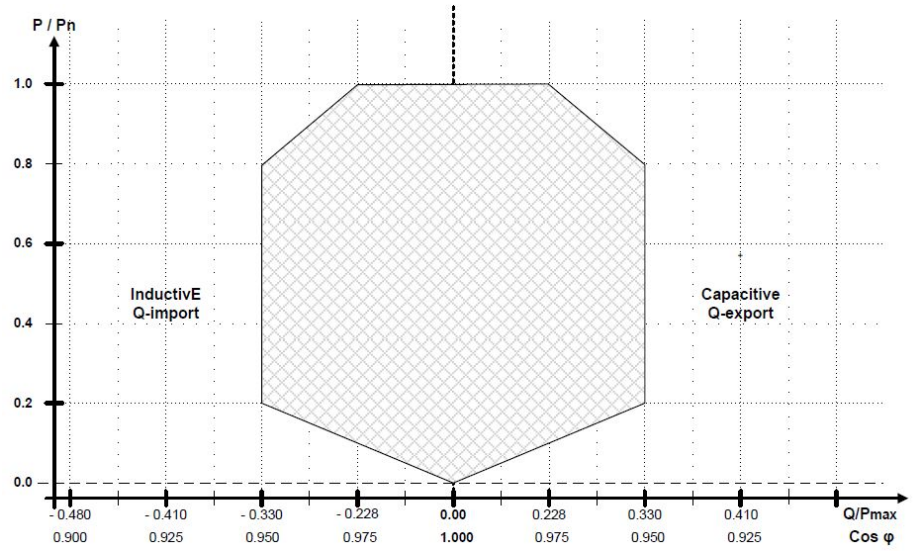

Figure 3.1: Reactive power requirement for wind power plants larger than 25 MW according to Energinet.dk's grid code [4]

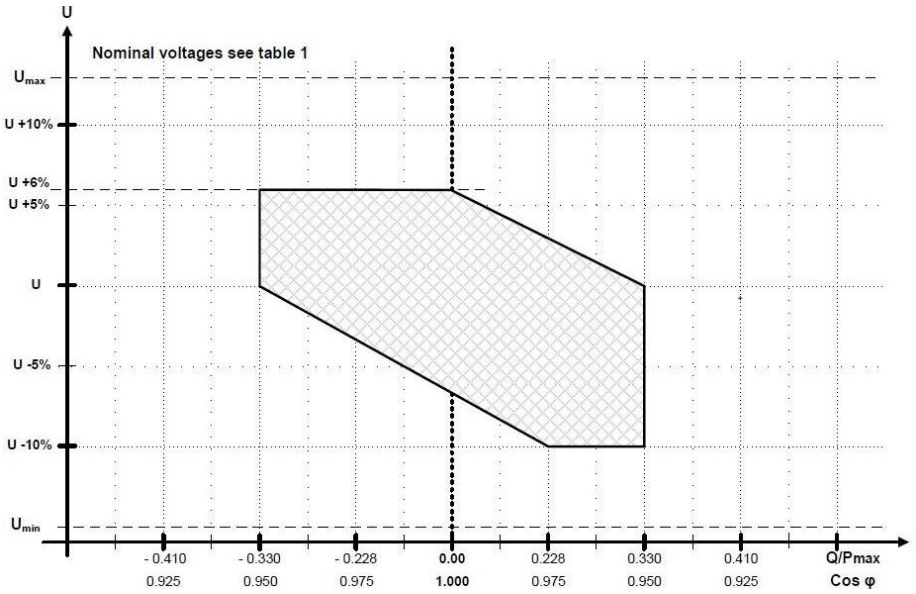

Figure 3.2: Voltage and reactive power requirements for wind power plants larger than 25 MW according to Energinet.dk's grid code [4]

Figure 3.1 shows the P-Q steady state requirements in form of the reactive power Q defined by the maximum active power P of a power plant or defined by the power factor (PF) as a function of the active power level from 0 pu to 1 pu (1 pu = P_{nom}). According to figure 3.1, wind power plants are required to have a reactive power capability over the power factor range between 0.95 leading to 0.95 lagging. Within the hashed area the wind power plant shall be capable of absorbing and generating reactive power and as illustrated, the area is divided into an inductive area for Q-import and a capacitive area for Q-export.
Figure 3.2 illustrates the voltage range related to the the wind power plant's reactive power requirements. The voltage is shown as a percentage of the nominal voltage at plant connection. The maximum range for reactive power capabilities, equal to the range in figure 3.1, is defined when the voltage at grid connection is 1 pu. Hence, at this voltage level, the wind power plant must be capable of moving within the full hatched area in 3.1. At a voltage setpoint of 1.06 pu, the wind power plant shall only be capable of absorbing reactive power and at voltage setpoint of 0.9 pu the wind power plant shall only be capable of generating reactive power. This is in compliance with the ENTSO-E grid code stating special requirement are allowed at high and low voltages. Above voltage V=1.06 pu and below V=0.9 pu, there are no reactive power requirements for the wind power plants in Denmark.

The reactive power capabilities of the 33 kV and 66 kV wind power plant investigated in this thesis are tested with simulations in Powerfactory and compared against the grid code requirements from Energinet.dk.

3.2 Reactive Power Capability

Electric energy is often transmitted, generated and used in AC systems. The apparent power S in AC circuit consists of the active power P and the reactive power Q. The apparent power is expressed in equation 3.1 [48].

$$|S| = \sqrt{|P|^2 + |Q|^2} \qquad [VA] \tag{3.1}$$

The apparent power is the magnitude of the complex power as expressed in equation 3.2 [48].

$$S = P + jQ \qquad [VA] \tag{3.2}$$

Reactive power, unlike active power, does not do any work. It can be expressed by equation 3.3 using the voltage V and the current I and the phase angle between voltage and the current $\phi = \delta - \beta$ [48]. δ represents the angle of the voltage and β represents the angle of the current. If β is less than δ, it is said

that the current lags the voltage and the load is inductive. If β is greater than δ, it is said that current leads the voltage and the load is capacitive. Reactive power is measured in Volt-Ampere-reactive VAr which has same dimensions as watts W.

$$Q = VI\ sin(\phi) \qquad [VAr] \tag{3.3}$$

The phase angle between the voltage and current is also used to define the power factor, as shown in equation 3.4 [48].

$$Power factor = \frac{P}{S} = cos(\delta - \beta) \tag{3.4}$$

Different components are capable of either absorbing or generating reactive power. In capacitive loads reactive power is produced and in inductive loads reactive power is absorbed. Table 3.1 gives an overview of some of the components in a power system that either produce or absorb reactive power [54]. As seen in the table, overhead power lines can both produce and absorb reactive power. This depends on the power line characteristic impedance referred to as the surge impedance $Z_c = \sqrt{\frac{L}{C}}$ where the surge impedance load SIL $= \frac{V_{nom}^2}{Z_c}$ [54]. The production or absorption of the overhead lines is decided by whether the overhead line is dominated by capacitance or inductance as indicated in table 3.1. The production and absorption of generators depends on whether the machine is over-excited or under-excited. When the generator is over-excited it generates reactive power and when the generator is under-excited the machine absorbs reactive power [3].

Table 3.1: Reactive power production and absorption of components

Component	**Q production**	**Q absorption**
Transformer		X
Cables	X	
Overhead line	X(capacitance)	X(inductance)
Synchronous generator	X(over excited)	X(under excited)
Harmonic filters	X	

The reactive power requirements set by Energinet.dk can be accomplished using different control options of the wind power plant. The components within a wind power plant that can be used to adjust the voltage are On Load tap changing substation transformers, dynamic and switch-able reactive power devices and wind turbines with reactive power capabilities [18].

For the 33 kV and 66 kV wind farm investigated in this project, the wind turbines are used for the reactive power control. It is the net reactive power flow that must meet the Q-requirements at grid connection, hence, the flow of reactive power through the wind power plant has to be considered.

The 33 kV and 66 kV wind farm are modelled with the Siemens 3.6 MW variable speed wind turbines. This turbine is equipped with a full load frequency converter which allows it to have control over a large power factor range. When the wind turbines are put in PV mode, from a load flow point of view, the wind turbine generators are able to control the active power and voltage magnitude injection into the wind farm. This also means that the wind turbines can control their import and export of reactive power by the active power production and the voltage set point of the wind turbines. The reactive power capability of the wind turbines is illustrated in figure 3.3 [42]. The reactive power capability when generating reactive power is shown as solid lines and when absorbing reactive power is shown as dotted lines for different voltage set points. A low voltage set point is able to generate more reactive power and a high voltage set point is able to absorb more reactive power.

If wind farms with reactive power capability of their wind turbines are unable to fulfil the Q-requirement in the grid code, the design of the WPP must be adjusted to compensate the remaining reactive power needed. Possible solutions that can be implemented or changed to provide the reactive power compensation needed are [18]:

- Adjusting the fixed transformer tap of substations transformers or wind turbine transformers.
- Adding (or adjusting the size of) a shunt reactor or capacitor bank.
- Changing the cables of the collection grid within the wind farm.
- Adding variable reactive power devices.

The dimensioning of a shunt reactor used as reactive power compensation for the 33 kV and 66 kV wind farm has been included in the research as a result of the reactive power capability investigation. The results and analysis of the investigation is presented in section 5.2. In addition to this, adjusting fixed transformer taps of the wind turbine transformers have also briefly been investigated, but here the main focus has been kept on the active power output and losses and the reactive power capabilities are evaluated as a subresult.

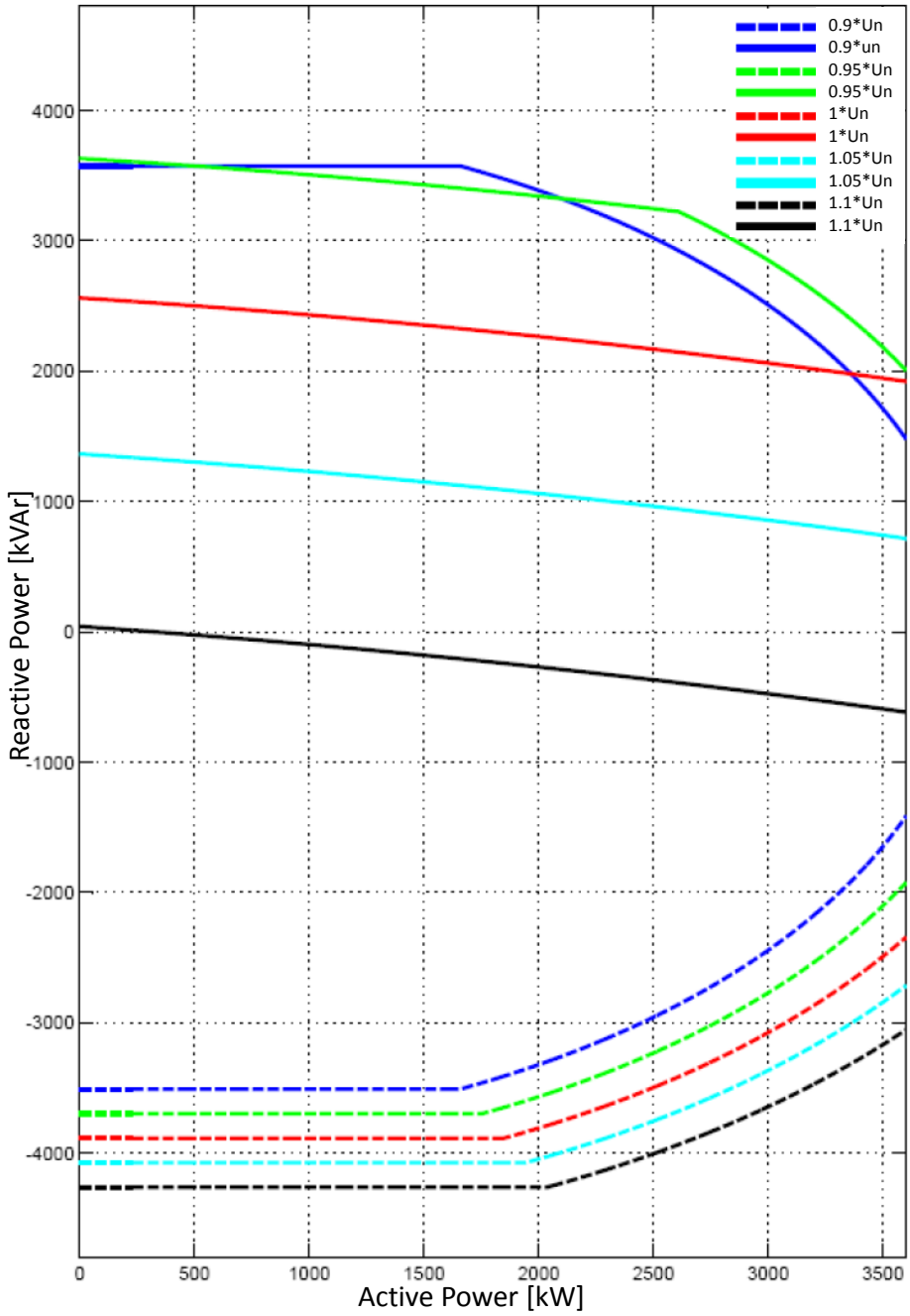

Figure 3.3: Reactive power capability of wind turbine [42].

3.3 Transformer Tap Changer

Power transformers are used in wind farms to convert the AC voltage and current into optimal level for economical power transmission. As the power is proportional to the product of the voltage and current, stepping up the voltage will lower the losses, since losses are proportional to current squared (I^2R) [48]. Hence, by stepping up the voltage from the wind turbine to the collection grid and again before the transmission to land, the losses can be reduced.
A transformer (trf) consist of a primary and secondary winding. A step up transformer increases the voltage from the primary side to the secondary side. For an ideal transformer the turns of the primary winding N_1 and the secondary winding N_2 are proportional to the voltage of the primary side V_1 and the secondary side V_2. Hence, the turns ratio α_t can be expressed by equation 3.5 [48]. For a step up transformer $\alpha_t < 1$ so the turns ratio will, for example, decrease if the voltage difference between the primary and secondary increases.

$$\alpha_t = \frac{N_1}{N_2} = \frac{V_1}{V_2} \tag{3.5}$$

Transformers can be equipped with tap changers allowing them to adjust the turns ratio. Tap changing transformers can be divided into two categories; On Load Tap Changers (OLTC) and De-Energized Tap Changers (DETC), the latter also known as Off Load tap changing transformers.

De-Energized tap changing transformers are only capable of changing the voltage setting when the transformer is not loaded. Some wind turbines are equipped with DETC [55] and can be used to for example optimize the active and reactive power flow, address unforeseen voltage issues in the design studies or adjust the wind farm to future changes in the grid [18] [50]. DETC have low maintenance cost and the difference in investment cost is minimal compared to a transformer not equipped with De-Energized tap changers [18] [21]. Figure 3.4 shows a basic example of a De-Energized tap changing transformer. The taps can be changed outside the transformer locking the new tap position into place. This is also valid for three phase transformers where all three phases are locked together only allowing the same tap position for all three phases. Majority of DETC have five tap positions, with two above normal operation and two below normal operation and a full tap range of $\pm 5\%$ [36] [27] [35]. This configuration is used for the wind turbines in the 33 kV and 66 kV wind farm modelled in Powerfactory.

On Load Tap Changers are able to regulate their voltage set point, hence the turn ratio, when the wind park is in operation. A wind farm's substation transformers are often equipped with OLTC [55]. They are mostly needed if there tend to be a large range of variations in the grid voltage and/or the wind turbines are limited in their ability to supply and absorb reactive power [18] [50].

Unlike the DETC, OLTC add a significant amount to the investment cost of substation transformer and have high-maintenance needs increasing the operation and maintenance cost [18]. Figure 3.5 shows an example of an on load tap changing transformer. The tap changers are often preferred on the high voltage winding as the current here is lower, hence, the tap changer contacts etc. can be smaller [37]. For all OLTC the essential part is that it allows voltage change of the transformer without interrupting the power circuit, hence, it is essential that the load current does not break during tap change.

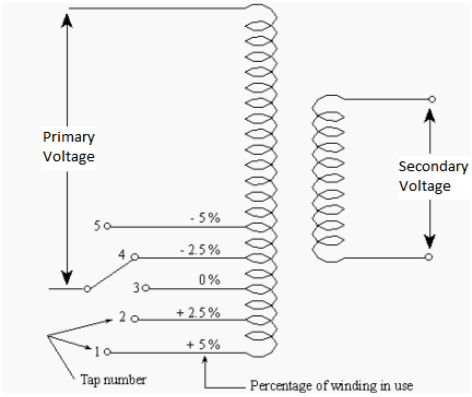

Figure 3.4: Basic example of an De-Energized tap changer transformer [36].

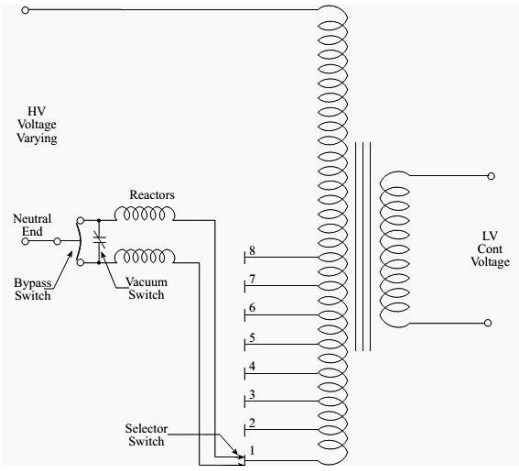

Figure 3.5: Example of an On Load tap changing transformer [37].

Generally OLTC have a maximum range of ±20% with individual tap between 0.8% and 2.5% [38]. The substation transformers in the 33 kV and 66 kV wind farm modelled in Powerfactory are equipped with tap changers with steps of 1.5% and a total range of ±15%.

Investigations have been conducted checking the benefits and withdrawals in terms of mainly active power losses but also reactive power flow when changing the taps of the wind turbine transformers in the 33 kV and 66 kV wind farm. The results and analysis of the investigation is presented in section 5.3.

3.4 Fault Cases

Equipment in a wind power plant can be exposed to insulation failure which can lead to heavy currents, also called short circuit (SC) currents [18]. As the magnitude of the short circuit currents are significantly larger than the normal operating current, there is a huge risk of damaging equipment during the fault. In order to avoid this, it is important to remove or disconnect the faulted section from the rest of the system. Switchgear (SG) is used as protective equipment where circuit breakers are designed to make, break and carry the short circuit current for a short time period. Therefore, one of the reasons to do a fault current investigations is to dimensioning switchgear in terms of its short circuit ratings. The short circuit rating of switchgear also has an impact on the cost of switchgear which is interesting to consider when comparing the switchgear requirement between the 33 kV wind farm and the 66 kV wind farm of this project [48] [72].

For a three phase circuit there are two main types of faults, symmetrical faults and unsymmetrical faults. The four common faults are briefly described in table 3.2. For unbalanced three phase systems, when calculating the associated current and voltages after a fault, the calculations can be simplified by transforming the unbalanced three phasors into three sets of balanced phasors known as the positive-, negative- and zero phase sequence networks. A more detailed description of the sequence network and SC faults is out of the scope for this project.

Short circuit simulations investigating the peak short circuit current for all four common faults at different locations in the 33 kV wind farm and the 66 KV wind farm have been carried out and the results are evaluated in section 5.4.

Table 3.2: Four common short circuit faults [48] [72] [62] [51]

Fault	Circuit Diagram	Fault Conditions	Description
Balanced three phase fault	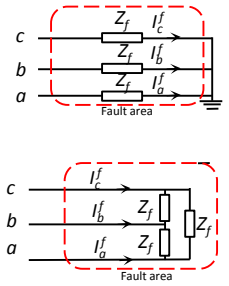	$I_a^f = I_b^f = I_c^f = 0$ Voltage phase *a* 3ø-ground $V_a^f = I_a^f Z_f$ Voltage phase *a* 3ø – clear of earth $V_A^f = \frac{1}{3} Z_f I_A^f$	Symmetrical fault. Balanced three phase faults can occur as a line to line to line ground fault or a line to line to line fault. Evaluated by the positive sequence network. Occur in 8% - 10% of SC fault cases.
Single line to ground fault	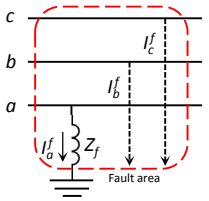	$I_b^f = I_c^f = 0$ $V_a^f = I_a^f Z_f$	Unsymmetrical fault. One phase comes in contact with ground. Evaluated by the zero, positive and negative sequence network connected in series. Occur in 75% - 80% of SC fault cases.
Double line to ground fault	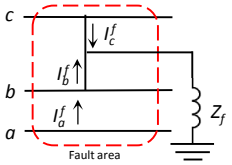	$I_a^f = 0$ $V_b^f = V_c^f = Z_f (I_b^f + I_c^f)$	Unsymmetrical fault. Two phases come in contact with each other and ground. Evaluated by the zero, positive and negative sequence network connected in parallel. Occur in 10% - 12% of SC fault cases.
Line to line fault	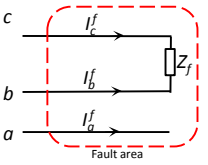	$I_a^f = 0$ $I_b^f = - I_c^f$ $V_b^f - V_c^f = I_b^f Z_f$	Unsymmetrical fault. One phase comes in contact with another phase. Evaluated by the positive and negative sequence network connected in parallel and the zero sequence network open circuit. Occur in 5% - 7% of SC fault cases.

Chapter 4

Model Design

Chapter 4 goes into details with the design of the models used to evaluate the technical performance of the 33 kV wind farm and the 66 kV wind farm in Powerfactory. The chapter briefly introduces the simulation tool Digsilent Powerfactory. The parameters of the components used in the model setup in Powerfactory is presented and differences between the 33 kV wind farm and 66 kV wind farm are shown. The model of the 33 kV wind farm is based on a generic wind farm model which is then modified for the 66 kV wind farm. Furthermore, the calculations associated with the sizing of the cables used in the 66 kV wind farm is presented in this chapter. Finally, the market availability of the components used in the 33 kV and the 66 kV wind farm is briefly discussed.

4.1 Digsilent Powerfactory

The simulation tool Digsilent Powerfactory is used to create the model of the two wind farms and to analyse the technical performance. Powerfactory written by Digsilent (DIgital SImulation for Electrical NeTwork) is an engineering tool used to model generation, transmission, distribution and industrial electrical power systems [12]. Powerfactory includes several simulation functions and for this thesis load flow simulations and short circuit simulations are made use of. One of the advantages of using Digsilent Powerfactory is its short simulation time making it possible to run many simulations with different criteria, for example, by making use of operation scenarios. In this thesis, the data obtained in Powerfactory has afterwards been transferred to and handled in Microsoft Excel. Digsilent Powerfactory provides a simple platform to set up a power system and, for this thesis, it has been a high advantage that general handling

of components in Digsilent Powerfactory is very user-friendly. Hence, changing or adding new components or adjusting parameters of component is a fast procedure to carry out.

Prior to conducting simulations the basics of Digsilent Powerfactory has been learned through tutorials available in Powerfactory and additional knowledge is mainly gained through Digsilent Powerfactory's own usermanual [9].

4.2 Powerfactory Model of the 33 kV and 66 kV Wind Farm

Summary of main similarities and differences between the two models

A generic wind farm with a 33 kV collection grid is compared to a wind farm with a 66 kV collection grid in Powerfactory. An overview of the main differences and similarities between the 33 kV wind farm and the 66 kV wind farm is captured in table 4.1. Section 4.2 and section 4.3 give a more detailed description of the wind farm models.

Table 4.1: Summary of main similarities/differences between the two Powerfactory models.

	33 kV wind farm	**66 kV wind farm**
Wind turbine	51*SWP 3.6MW	51*SWP 3.6MW
Wind turbine transformer	0.69/33 kV	0.69/66 kV
Collection grid voltage	33 kV	66 kV
Collection grid cable A	$150mm^2$ I=396A R=0.14Ω/km Total length=38.9km	$95mm^2$ I=300A R=0.23Ω/km Total length=42.1km
Collection grid cable B	$500mm^2$ I=716A R=0.06Ω/km Total length=6.8km	$150mm^2$ I=375A R=0.146Ω/km Total length=3.6km
Substation transformer	33/132 kV	66/132 kV
Sea-to-land cable	length 47.8km V=132kV	length 47.8km V=132kV

Model design

The 33 kV wind farm is built in Powerfactory using standardised components based on an existing project library provided by Siemens Wind Power. The 66 kV wind farm is a modified version of the 33 kV wind farm where the size of cables, the wind turbine transformers and substation transformers are changed to fit the 66 kV level in the collection grid.

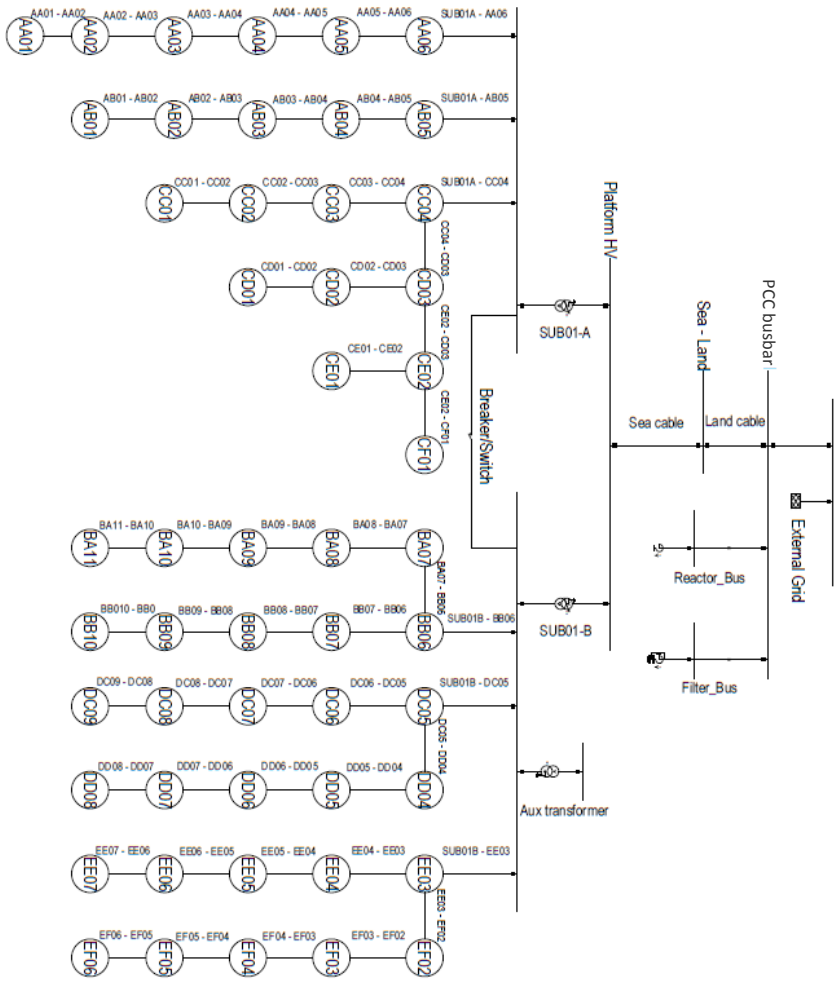

Figure 4.1: Layout of wind farm as designed in Powerfactory

Hence, both wind farms have the same layout which is shown in figure 4.1. All the wind turbines consist of a generator, filters and a transformer. An example of a wind turbine is shown in figure 4.2 representing wind turbine AA01.

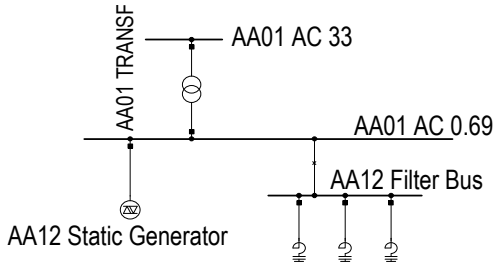

Figure 4.2: Layout of wind turbine AA01 in Powerfactory. All wind turbines in the model are designed in a similar way.

The layout of the wind farms, in terms of number of wind turbines in an array, number of turbines connected to each substation and the length of the cables, has been predetermined using a standardised model provided by Siemens Wind Power. It is therefore assumed that this layout is a well representative model of a real offshore wind farm.

The point of common coupling (PCC), the location where the public network is entered, is chosen to be after the sea cable and land cable at the PCC busbar. At PCC the results of all load flow simulations carried out are recorded as generally up until PCC the wind farm operators are accountable for the losses and only the power delivered after PCC is paid for [34]. The overall specifications of the two wind farms are summaries in table 4.2.

Table 4.2: General information about the 33 kV and the 66 kV wind farm.

Total wind power plant capacity	183.6 MW
Total number of wind turbines	51
Size of wind turbines	3.6 MW
Number of substation transformers	2
Size of substation transformers	180 MVA
Size of wind turbine transformers	4 MVA
Length of cables between wind turbines in the internal grid	0.562 km - 2.321 km (majority are 0.858 km)
Distance from offshore substations to PCC	47.8 km
Voltage level at PCC	132 kV
Nominal operating frequency	50 Hz

The wind turbines modelled in Powerfactory consist of a static generator connected to a turbine transformer and a harmonic filter. The wind turbines modelled are the Siemens 3.6 MW. It is equipped with a full-size converter, which control the behaviour of the wind turbine as seen from the grid side, and can therefore be modelled as a static generator in Powerfactory. The wind turbine has an apparent power of 4 MVA with a power factor of 0.9. The turbines are modelled with PV control and the capability curve of the Siemens 3.6 MW turbine have been specified in the Powerfactory model.

For the simulations conducted in Powerfactory, the harmonic filters are only of interest in term of their active and reactive power consumption. When running a load flow, the turbine filters produce 0.08 MVAr reactive power, hence, affecting the reactive power capability of the wind farm and consume 0.4 kW of active power. A harmonic filter is also connected at the point of common coupling. This harmonic filter consumes 1.4 MW, hence, increasing the active power loss while it produce 27 MVAr reactive power also affecting the reactive power capability of the wind farm. As the harmonic filters will affect the results of the simulations, they are kept as components in the wind farm and the exact same harmonic filters used in the 33 kV wind farm are duplicated into the 66 kV wind farm.

As the collection grid voltage is different in the 33 kV and the 66 kV wind farm the same wind turbine transformer cannot be used as the high voltage level of the transformer will be different. To be able to make a good comparison between the two wind farms, it has been decided to use the 33 kV wind farm's wind turbine transformer as base component and only change the high voltage level of the transformer in the 66 kV wind farm. A more detailed description of the wind turbine transformers is summarised in table 4.3.

Table 4.3: Specification of the wind turbine transformers in both wind farms modelled in Powerfactory.

	33 kV wind farm	**66 kV wind farm**
Rated power	4 MVA	4 MVA
Rated voltage HV side	33 kV	66 kV
Rated voltage LV side	0.69 kV	0.69 kV
Configuration	DYN11 *30deg	DYN11 *30deg
Positive seq. impedance SC voltage uk	6%	6%
Copper losses	34 kW	34 kW
Tap changer	0/-2/2 (neutral=0)	0/-2/2 (neutral=0)
Additional voltage per tap LV side	2.5%	2.5%

Similar assumptions have been made in terms of the substation transformers where the voltage on the LV side of the transformers will be different. Table 4.4 gives a summary of the substation transformers modelled in Powerfactory.

Table 4.4: Specification of the substation transformers in both wind farms modelled in Powerfactory.

	33 kV wind farm	**66 kV wind farm**
Rated power	180 MVA	180 MVA
Rated voltage HV side	132 kV	132 kV
Rated voltage LV side	33 kV	66 kV
Configuration	YNd1	YNd1
Positive seq. impedance SC voltage uk	10.5%	10.5%
Copper losses	517.5 kW	517.5 kW
Tap changer	11/1/21 (neutral=11)	11/1/21 (neutral=11)
Additional voltage per tap HV side	1.5%	1.5%

The cables used in the 33 kV wind farm model are from the standardised model provided by Siemens Wind Power. A check of the cables sizes have been carried out and no need for changing them was found. Two cable sizes are used in the collection grid and a third size is used for the connection between the transformer substations and PCC. A summary of the cables is given in table 4.5.

Table 4.5: Specification of cables in the 33 kV WF modelled in Powerfactory.

		Cable A	**Cable B**	**Sea-to-land cable**
Nominal cross section	[mm^2]	150	500	800
Rated voltage	[kV]	33	33	132
Rated current	[A]	396	716	795
Total length of cable	[km]	38.9	6.8	47.8
Resistance (pos/neg seq.)	[Ω/km]	0.14	0.06	0.05
Reactance (pos/neg seq.)	[Ω/km]	0.12	0.1	0.05
Resistance (zero seq.)	[Ω/km]	0.51	0.34	0.15
Reactance (zero seq.)	[Ω/km]	0.1	0.09	0.07
Capacitance (pos/neg seq.)	[μF/km]	0.195	0.318	0.223
Capacitance (zero seq.)	[μF/km]	0.23	0.34	0.223
Conductor material		Copper	Copper	Copper

4.3 66 kV Collection Grid Cables

The cross section of cables is closely related to the current rating of a cable. As the current of the cable is different in the 66 kV wind farm compared to the 33 kV wind farm due to the higher voltage level, the cables in the 66 kV wind farm have been designed to fit the 66 kV voltage level.

The cables for the 66 kV wind farm are designed using ABB datasheet for submarine cables [17]. The datasheet can be found in appendix A.1, where the used sections are highlighted. The datasheet shows the current rating related to the cross section for three-core submarine cables together with the capacitance and inductance for all cables at different voltage ratings. Hence, the first step to design the cables is to establish what current ratings are needed for the collection grid cables in the 66 kV wind farm.
The current per phase I of a cable depends on the voltage V and the apparent power S of the cable as expressed in equation 4.1 [61]. The apparent power varies with the number of wind turbines connected in a row ranging from 1 wind turbine = 4 MVA to 10 wind turbines = 10WT*4 MVA = 40 MVA. No rows with 7, 8 or 9 wind turbines exists, as seen on the layout of the wind power plant in figure 4.1.

$$I = \frac{S}{\sqrt{3} * V} \tag{4.1}$$

By calculating the current on the collection grid cables using equation 4.1, it is found that for up to 6 wind turbines connected in row, the current on the cable does not exceed 300 A. Hence, the ABB cable with the lowest cross section of 95mm^2 can be used as the rated current of this cable is 300 A. The three cable sections which connect 10 wind turbines to substation B have a current rating of 350 A calculating with equation 4.1. The ABB cable with a rated current of 375 A and a cross section of 150mm^2 have therefore been chosen for these three cable sections.

The capacitance and inductance of a 95mm^2 66 kV three core cable and of a 150mm^2 66 kV three core cable are given in the ABB datasheet, see appendix A.1. However, the resistance must be calculated. The DC resistance of a cable can be calculated according to equation 4.2. Here, ρ is the resistivity of the conductor material which in this case is copper, l is the length of the cable, A is the cross sectional area, α_0 is the temperature coefficient and T is the temperature [72] [58]. As the wind farm is operating in AC and not DC, the AC resistance should be calculated, which is given by 4.3. Here, γ_s is a measure of the skin effect and γ_p is a measure of the proximity effect [72] [58].

However, when calculating the AC resistance it showed that $\gamma_s \ll 0$ and $\gamma_p \ll 0$ and therefore did not have any significant effect on the AC resistance for the desired precision. For this reason, the skin effect and proximity effect have been neglected.

$$R_{DC} = \frac{\rho l}{A}\left(1 + \alpha_0(T_\Theta - T_0)\right) \tag{4.2}$$

$$R_{AC} = R_{DC}\left(1 + \gamma_s + \gamma_p\right)) \tag{4.3}$$

The resistance calculated and the capacitance and inductance obtained from the ABB datasheet is for the positive and negative sequence. For zero sequence it has been assumed that the capacitance and inductance remain the same. It is also seen on the cables used in the 33 kV wind farm that the capacitance and inductance are in the same order comparing the positive and negative sequence to the zero sequence. However, this is not the case for the resistance which as a rule of thumb is three times larger in the zero sequence network compared to the positive and negative sequence [1]. This is also seen on the cables in the 33 kV wind farm. Hence, the zero sequence resistance of the collection grid cables in Powerfactory for the 66 kV wind farm are three times higher compared to the calculated resistance used for the positive and negative sequence.
The same cable from the substation to PCC used in the 33 kV wind farm is also implemented in the 66 kV wind farm model and is described in table 4.5. A summary of the collection grid cables in the 66 kV wind farm can be found in table 4.6.

Table 4.6: Specification of collection grid cables in the 66 kV wind farm modelled in Powerfactory.

		Cable A	**Cable B**
Nominal cross section	[mm^2]	95	150
Rated voltage	[kV]	66	66
Rated Current	[A]	300	375
Total length of cable	[km]	42.1	3.6
Resistance (pos/neg seq.)	[Ω/km]	0.23	0.146
Inductance (pos/neg/zero seq.)	[mH/km]	0.44	0.41
Resistance (zero seq.)	[Ω/km]	0.69	0.44
Capacitance (pos/neg/zero seq.)	[μF/km]	0.17	0.19
Conductor material		Copper	Copper

Two different cables are used in the collection grid of the 66 kV wind farm. The most used cable is 95mm^2 with a total length of 42.1 km. The other cable is 150mm^2 with a total length of 3.6 km. The cross sectional area of this cable is the same as cable A in the collection grid of the 33 kV wind farm, however, cable A in the 33 kV model is from the standardised model provided by Siemens Wind Power. Despite this, the parameters of the 150mm^2 ABB cable used in the 66 kV wind farm are very similar to the parameters of cable A in the 33 kV model. The small differences can be caused by different cable manufacturer.

4.4 Market Availability of Components

An important aspect to keep in mind when comparing the two cases is the availability of the components on the market today. It is easy to simulate 66 kV components in Powerfactory but for wind farm operators to choose to use 66 kV in offshore wind farms also depends on whether a supply chain for 66 kV components exists.

Switchgear and transformers that can be used in 66 kV offshore wind farms are currently available on the market today. Although some of the solutions are not identical in the set up of the 33 kV components, there are 66 kV switchgear and transformers technologically ready for implementation [64] [15] [16].

The technological readiness of 66 kV sea cables are, however, still in the development stage. Generally, offshore wind farms use wet type cables that use XLPE or EPR to block water which, compared to dry type cables, do not need to incorporate a water blocking lead sheath. The wet type cables are used as they are less expensive compared to dry type cables, however, currently only wet type cables up to 33 kV are readily available on the market today [64]. In order to move the development of 66 kV sea cables, the Carbon Trust's Offshore Wind Accelerator launched a competition "the Race for 66 kV" in 2013 to find cable manufacturers that can develop and qualify cables to be used in 66 kV wind farms [15] [28]. Since 2014, three manufacturers (Nexans, Prysmian and JDR) have been moving forward with the development of cables for 66 kV offshore wind farms with the help of funds from Carbon Trust's Offshore Wind Accelerator. The commercial availability of the wet type cables are expected to be available in 2017 [11].

Chapter 5

Simulations, Analysis and Results

Chapter 5 presents the results of the simulations carried out in Powerfactory and further evaluated using Excel. The set up of the simulations are briefly explained for each technical evaluation and the results are analysed and presented in forms of figures and tables. The technical performance of the 33 kV and 66 kV wind farm is evaluated and presented in this chapter in terms of active power losses, reactive power capabilities, fault current in different fault cases and the impact of using wind turbine tap changing transformers. The active power loss evaluation includes energy losses for the two wind farms at Horns Rev and Hvide Sande as well as the efficiency of both wind farms. In addition to this, the distribution of losses for the components in the two cases is evaluated and compared. The reactive power capabilities of both wind farms are found for different scenarios and the overall reactive power compensation needed in the two cases is estimated in order to fulfil the Danish grid code requirements. The effect of using tap changers on the wind turbine transformer are evaluated mainly in terms of active power losses where the optimal tap position is found. The results of the fault analysis are equally presented in terms of the peak short circuit current for different fault cases and differences between the 33 kV wind farm and the 66 kV wind farm are analysed. Furthermore, this chapter includes an economic evaluation of the 33 kV and the 66 kV wind farm in terms of installation cost of relevant components based upon design parameters and technical performance as well as cost of energy losses. The economic results are discussed in relation to the cost of energy for the wind farms. Finally, in the last section, an overall comparison of the technical performance and economic evaluation between the 33 kV and the 66 kV wind farm are presented and discussed and the results are put into perspective by comparing the work in this thesis with literature of similar investigations.

5.1 Active Power Loss

In the evaluation of active power losses of both wind farms load flow simulations have been carried out in Powerfactory and the active power output of the wind farms have been recorded at PCC. Operation scenarios have been set up where each scenario represents a different dispatched active power set point at the wind turbines following the power curve in figure 2.2. The voltage set point at the wind turbines and at the grid is set to 1 pu for all scenarios. All 51 wind turbines are active and filters at each wind turbine and at the grid connection are connected as they carry a small power loss. The shunt reactor at grid connection, used as reactive power compensation, is disconnected as the dimensioning of the needed reactive compensation is evaluated separately. Its impact in terms of active power losses will be briefly discussed in the section 5.6. The exact same scenarios are set up in the 33 kV and the 66 kV wind farm and the active power output recorded at PCC is further analysed in Excel.

In general, the losses are proportional to the current squared and the power is proportional to the product of current and voltage. The initial hypothesis is therefore, that the losses in the 66 kV wind farm will be significantly lower than the losses in the 33 kV wind farm due to double the voltage level. In both cases, the active power losses will increase with increased dispatched power. To get a more precise loss estimation, the total losses in the wind farms are calculated taking the Weibull distribution into account. Hence, the operation scenarios in Powerfactory are defined to represent the dispatched power at each wind speed. The total yearly energy output of the wind farm, before losses are substracted, is then calculated by equation 5.1, where Δt represents the time period, P_u^{out} is the active power at PCC for wind speed u and σ_u is the probability of the wind speed u. The total energy losses are calculated using equation 5.2, where $P_u^{WT\,out}$ is the dispatched active power of each wind turbine at wind speed u.

$$E_{total} = \Delta t * \sum_{u=0-25m/s} \left(P_u^{out} * \sigma_u\right) \tag{5.1}$$

$$E_{loss} = \left(\Delta t * \sum_{u=0-25m/s} \left(51 * P_u^{WT\,out} * \sigma_u\right)\right) - E_{total} \tag{5.2}$$

The average dispatched active power related to the capacity factor of Horns Rev and Hvide Sande, as calculated in section 2.2, has also been included as a scenario, where the total yearly energy output, before losses are substracted, is calculated by $P_{CF\,average} * 8760h$. A comparison between using the capacity factor and the full power curve to calculate the energy output and energy losses is made.

The results of yearly energy losses obtained by analysing the data from the load flow simulations for both the 33 kV wind farm and the 66 kV wind farm are illustrated and compared in figure 5.1.

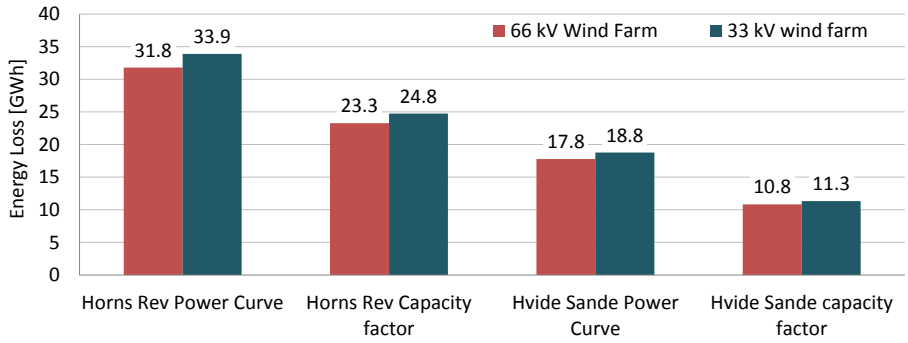

Figure 5.1: Energy loss of the 33 kV and 66 kV wind power plant over a time period of 1 year at Horns Rev and Hvide Sande.

As illustrated in figure 5.1, the losses are different when calculated over the range of the power curve compared to using the average dispatched active power related to the capacity factor for both Horns Rev and Hvide Sande. This is also expected, as the losses varies with the dispatched active power. The losses are lower at Hvide Sande compared to Horns Rev but this should be evaluated in relation to the yearly energy output of the wind farms. The yearly energy production is for example for the 33 kV wind farm calculated using the range of the power curve 563 GWh at Hvide Sande and 910 GWh at Horns Rev. This difference is due to the Weibull distribution at the two sites as the probability of lower wind speeds is higher at Hvide Sande and the losses are lower at lower wind speeds. Hence, as mentioned in chapter 2.2, the Weibull distribution is very important to evaluate when choosing the correct wind turbine for a site. As Horns Rev is a better location for the Siemens 3.6 MW wind turbines, Hvide Sande has been disregarded in the coming analysis of the 33 kV wind farm and the 66 kV wind farm.

Figure 5.1 shows that in all cases the yearly energy loss is lower in the 66 kV wind farm compared to the 33 kV wind farm, as initially expected. This can also be confirmed when looking at the efficiency of the wind farms at different active power penetration in figure 5.2. At nominal power the efficiency is roughly 1.5% higher in the 66 kV case compared to the 33 kV case.

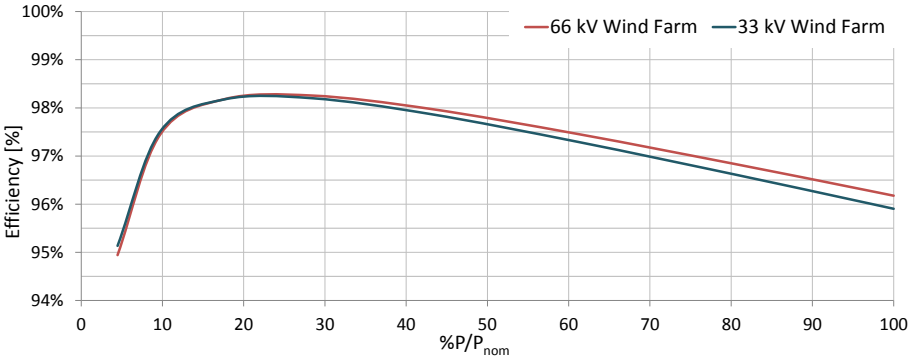

Figure 5.2: Efficiency at different dispatch active power levels for the 33 kV wind farm and 66 kV wind farm.

When comparing the total energy losses between the two wind farms at Horns rev for the whole power curve range, the losses in the 66 kV wind farm only decrease with 6%. The reason for the relatively low loss reduction when using 66 kV instead of 33 kV can best be explained through further investigation considering the distribution of losses in the two wind farms.

Figure 5.3 shows the loss distribution of different components in both wind farms and figure 5.4 shows the increase or decrease in energy losses of different components when going from the 33 kV wind farm, set as the reference case, to the 66 kV wind farm.

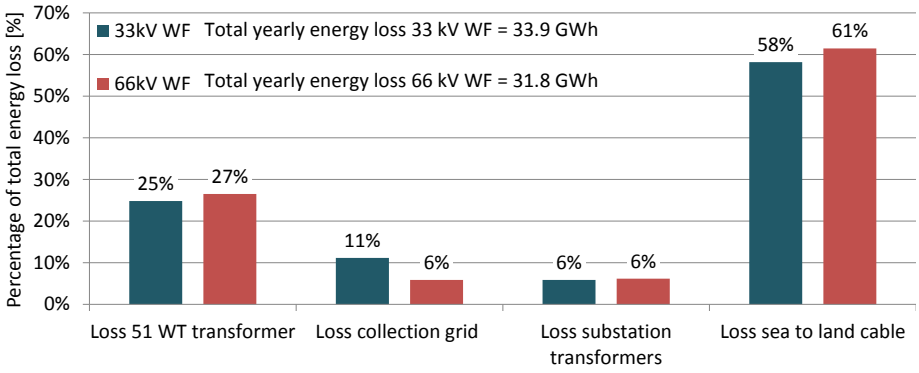

Figure 5.3: Distribution of the yearly energy losses in the 33 kV and the 66 kV wind farm

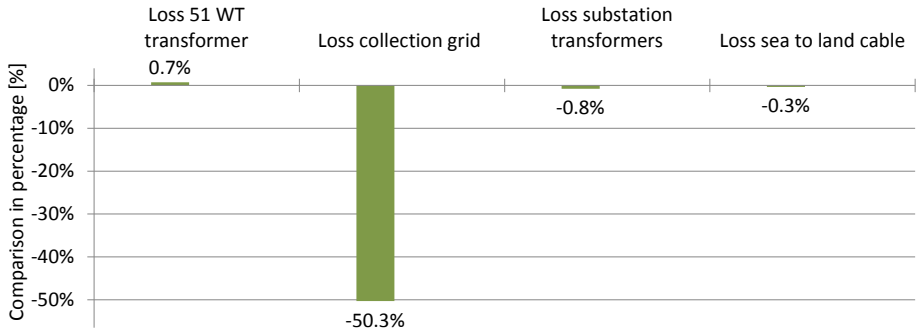

Figure 5.4: The energy loss in the 33 kV wind farm compared to the 66 kV wind farm for different components in the collection grid. A positive value relates to an increase in losses and a negative value relates to a decrease in losses when moving from 33 kV to 66 kV

The results are obtained through load flow simulations where 6 different wind speeds and their associated dispatched active power from the power curve have been used as input. The Weibull distribution of Horns Rev has then been used to calculate the losses in the two wind farms. The losses have been found for the wind turbine transformers, the collection grid cables hence the cables in the wind turbine arrays to the substation transformers, the two substation transformers and the sea-to-land cable.

Figure 5.3 shows a similar distribution of losses of the components in both the 33 kV and the 66 kV wind farm. The largest loss of around 60% comes from the sea-to-land cable, which is caused by the long length of this cable. This is also why the wind farm's distance to shore is very important to consider when planning new offshore wind farms. The main difference in the distribution of losses in the two wind farms are in the collection grid cables. The improvement in the collection grid losses when using 66 kV instead of 33 kV is 50% and only very small loss variations ($<$1%) occur in the transformers and the sea-to-land cable as seen on figure 5.4. The improvement of losses in the collection grid cables in the 66 kV wind farm are caused by the increase in voltage. As the power of the cables is proportional to the product of the voltage and current and the power is the same in both cases, when the voltage increase with a factor 2, from 33 kV to 66 kV, the current will be halved. The losses in the cable can be calculated according to equation 5.3.

$$P_{loss} = I^2 R \tag{5.3}$$

Hence, I^2 will decrease with a factor 4 when moving from 33 kV to 66 kV. However, the losses in the 66 kV collection grid cables are not 1/4 of the losses in the 33 kV collection grid cables as the resistance of the cables also has to be taken into consideration. Due to the smaller cable size used in the 66 kV collection grid cables, the resistance of these cables is larger compared to the cables of the 33 kV collection grid. The resistance of the cables in the two cases have been calculated according to the specification of the cables in table 4.1 in section 4.2. The results of the calculations showed that the resistance of the cables in the 66 kV wind farm increases with 1.75 compared to the 33 kV wind farm. The losses in the collection grid cables of 66 kV wind farm should therefore be $\frac{1}{4} * 1.75 = 44\%$ of the losses in the collection grid cables of the 33 kV wind farm. The actual decrease obtained in Powerfactory (=50%) is slightly higher, however, the difference can probably be explained by the choice of load flow simulations carried out and how the data from the load flow simulation is handled, e.g. rounding of numbers.

A 50% decrease in the collection grid cable loss is very large but when considering the distribution of losses (figure 5.3) the collection grid cables only represent 11% of the total losses in the 33 kV wind farm and 6% of the total losses in the 66 kV wind farm. Therefore, the decrease in losses when using 66 kV instead of 33 kV in the collection grid of the wind farms investigated is only 6%.

The active power losses have also been investigated under the conditions used in the reactive power simulations discussed in section 5.2, where the external grid voltage change between 0.9 and 1.06 pu and the wind turbines' voltage set point change between 0.9 pu to 1.1 pu. For all scenarios, the active power losses are always lower in the 66 kV wind farm compared to the 33 kV wind farm in the range between 0.3-11% lower.

Hence, the comparison of energy losses between the 33 kV and the 66 kV wind farm confirms the expectations in the initial hypothesis of lower losses in the 66 kV case. However, the overall loss evaluation only showed a low improvement in the energy losses when using 66 kV instead of 33 kV.

The cost of energy losses and how the energy losses affect the annual energy production in both wind farms are evaluated in section 5.5.

5.2 Reactive Power Capability

The reactive power capabilities of the two wind farms have been investigated using load flow simulations in Powerfactory. Simulations have been conducted for various conditions considering the full range of the grid voltage set point for Q-requirements, the full WT voltage range and the full dispatched active power range of the wind turbines. This is in accordance to the tests suggested by [18]. The reactive power Q absorbed or produced by the two wind farms have been recorded at PCC for a voltage set point at the wind turbines of 0.9 pu and 1.1 pu for dispatched active power at the wind turbines adjusted between 0-100%. The WT voltage set points are chosen, in order to use the full range of the reactive power capabilities of the wind turbines. The results of the simulations have been compared to the Q-requirements in the Danish grid code. The absorption of Q at PCC can be seen by the main network as a connection of inductance into the network to help lower the grid voltage and the production of Q at PCC can be seen as a connection of a capacitor into the main network to help raise the grid voltage.
Figure 5.5 shows the results of the load flow simulations when the voltage set point of the external grid is 1 pu, in figure 5.6 the voltage set point is 0.9 pu and in figure 5.7 it is 1.06 pu. In the three figures 5.5, 5.6 and 5.7 the Danish grid code requirements are also represented. The load flow simulations are carried out while the shunt reactor, which can be used as reactive power compensation, is disconnected as one of the aims of the reactive power investigation is to calculate and compare the needed compensation in the two wind farms.

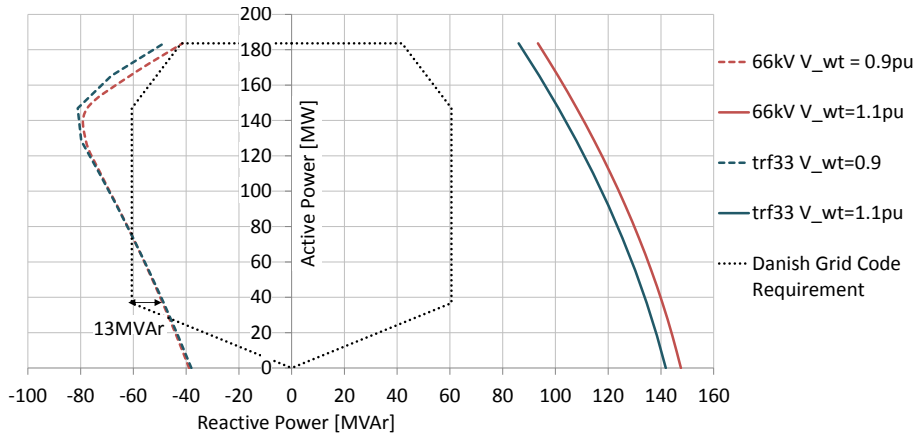

Figure 5.5: Reactive power capability of the 33 kV wind farm and the 66 kV wind farm measured at PCC when the external grid voltage is 1 pu.

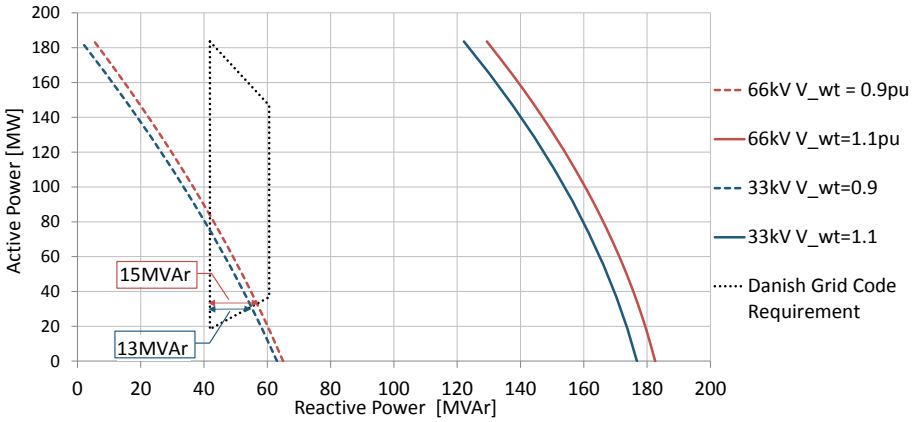

Figure 5.6: Reactive power capability of the 33 kV wind farm and the 66 kV wind farm measured at PCC when the external grid voltage is 0.9 pu which relates to the minimum voltage requirement that a wind farm must provide reactive power support according to the Danish grid code.

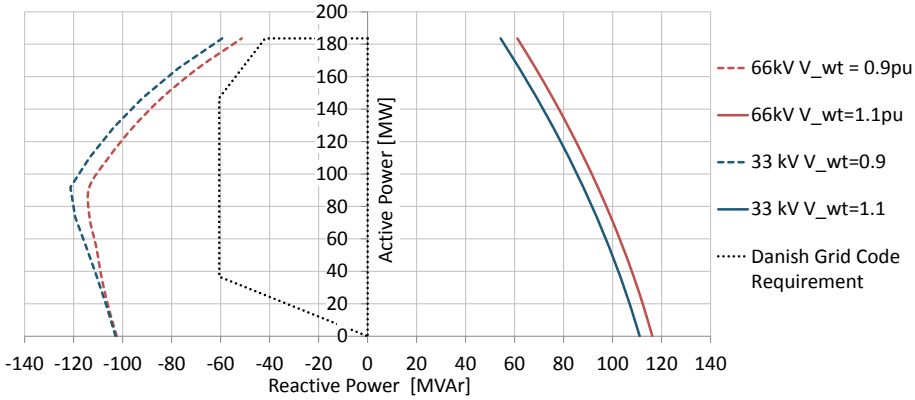

Figure 5.7: Reactive power capability of the 33 kV wind farm and the 66 kV wind farm measured at PCC when the external grid voltage is 1.06 pu which relates to the maximum voltage requirement that a wind farm must provide reactive power support according to the Danish grid code.

The control of reactive power in the wind farms is carried out by using the reactive power capabilities of the wind turbines. The actual reactive power capability of the wind turbines needs to be seen in relation to the rest of the wind farm and grid. The wind turbines are capable of adjusting their reactive power production and absorption according to the capability curve (in figure 3.3) and their final set point depends on voltage of the wind farm and the reactive power losses (absorb or produce) throughout the wind farm. Therefore, if, for example, the grid voltage set point changes, the maximum reactive power produced or absorbed by the wind turbines and wind farm will vary. Figure 5.5, 5.6 and 5.7 illustrate the production of Q from the wind farm as positive numbers and the absorption of Q as negative numbers. As seen on the figures, the higher grid voltage the lower maximum reactive power are both wind farms able to produce and the more are they able to absorb.

The configuration of the wind turbines in Powerfactory, for the simulations conducted, are a voltage set point of 0.9 pu or 1.1 pu. However, when running the load flow simulations, the voltage set point of the wind turbines is not in all cases kept, as the minimum or maximum reactive power has been reached. It is noted on the figures that some of the reactive power curves bends when reactive power is absorbed. The bend occurs as the wind turbines have reached their maximum reactive power (leading) capabilities and as seen on the the reactive power capabilities of the wind turbines in figure 3.3, at higher dispatched power the absorption of Q decreases causing a bend in the graph.

Figure 5.5, 5.6 and 5.7 show that the two wind farms for all three voltage set points at PCC are capable of producing the reactive power required to fulfil the Danish grid codes. However, in the case of the grid voltage = 1.06 pu (figure 5.7), the wind farms would need to absorb reactive power in order to contribute to lowering the voltage in the grid and that the wind farms are able to produce reactive power under these conditions is therefore irrelevant.
For two of the voltage set points at PCC (V = 1 pu and V = 0.9 pu) both wind farms are incapable of absorbing the reactive power required by the Danish grid code at all dispatched power levels. If the voltage at the grid is 1 pu (figure 5.5), when the dispatched active power of the entire wind farm is between 25 MW and 75 MW the wind farms need additional reactive power absorption. As illustrated on figure 5.5, the additional reactive power absorption needed is 13 MVAr for both the 33 kV and the 66 kV wind farm.
Similarly, if the external grid voltage is 0.9 pu (figure 5.6), the wind farms also need an additional inductive reactive power compensation in order to fulfil the Danish grid code. Under these conditions, the additional inductive reactive power compensation needed is 13 MVAr for the 33 kV wind farm and 15 MVAr for the 66 kV wind farm.

The reactive power capabilities of the wind farms at PCC are a result of all the components in the WPP. That both cases need inductive Q-compensation is caused by the production of reactive power in the cables and in the harmonic filters. Particularly, the long sea-to-land cable produces a large amount of reactive power which therefore, in some situations, must be compensated in order to fulfil the grid code requirements.

The additional inductive reactive power needed can be compensated by using a shunt reactor connected at PCC. A shunt reactor absorbs reactive power. It can either be permanently connected or connected through a circuit breaker and then switched in and out. The shunt reactor in the two wind farms is switchable. The size of the shunt reactor should be 13 MVAr in the 33 kV wind farm and 15 MVAr in the 66 kV wind farm.

The differences in the reactive power capabilities between the two wind farms can be explained by considering the reactive power flow through the wind farms. The production of reactive power in cables depends on the voltage squared [39]. As the voltage is doubled in the 66 kV wind farm, the production of reactive power from the cables in the collection grid is higher compared to the 33 kV wind farm. The reactive power absorption of the transformers is also dependent on the voltage [39]. This results in higher reactive power absorption by the transformers in the 66 kV wind farm. However, the difference in reactive power flow between the two wind farms is largest in the cables compared to the transformers. This was verified through extended simulations investigating the reactive power flow through different components in the wind farms. Therefore, as a result of the enhanced Q production in the collection grid cables, the 66 kV wind farm is capable of producing more but absorbing less reactive power compared to the 33 kV wind farm.

All in all, figure 5.5, 5.6 and 5.7 show that the 66 kV wind farm is able to produce around 6 MVAr more than the 33 kV wind farm but is able to absorb between 0-2 MVAr less. Overall, both wind farms are able to produce the necessary reactive power to fulfil the grid code requirements and they both need inductive reactive power compensation. The needed inductive reactive power compensation is 2 MVAr higher in the 66 kV case compared to the 33 kV case.

The estimated cost of the reactive power compensation needed in the 33 kV wind farm and the 66 kV wind farm has been calculated and compared in section 5.5.

5.3 Tap Changing Transformer Effect on P & Q

So far, the technical performance of the two wind power plants have only been investigated using fixed tap settings of the transformers. It is, however, possible to configure the wind turbine transformers and/or the substation transformers with the aim of obtaining a better performance of the wind power plants.
The wind turbine transformers and substation transformers used in Powerfactory are all equipped with tap changing functions. The wind turbine transformer has 5 taps from -2 to 2, with 0 being neutral position. The additional voltage per tap is 2.5%. In the model, the tap changers are equipped on the low voltage side. Therefore, a tap setting of for example tap -1 will decrease the turns ratio by 2.5% (see equation 3.5 in section 3.3) while a tap setting = 1 will increase the turns ratio with 2.5%. The wind turbine's taps are De-Energized tap changers, hence, the cost of the transformer with or without the taps are similar in price. Therefore, if the technical performances are improved using the taps on the wind turbine transformers it is assumed that it would not increase the investment cost of the wind turbine transformers.
The two substation transformers have 21 taps from 1 to 21 where tap 11 is the neutral position. The additional voltage per tap is 1.5%. As the tap changers are configured on the HV side, taps > 11 will decrease the turns ratio while taps < 11 will increase the turns ratio of the transformer. The substation transformers are built with OLTC. Hence, the implementation of tap changers on the substation transformers would significantly increase the investment cost.

Due to the assumptions of the cost impact, that implementing taps have on the wind turbine and the substation transformers, the investigation of using tap changers have been focused on the WT transformers. The use of the taps on the substation transformers has only briefly been evaluated in regards to further optimisation following the investigation of WT tap changing transformers.
The main investigation have been focused on finding the optimal WT tap position in terms of active power losses of both wind farms. In addition to this, the reactive power flow has been investigated at the optimal WT tap position for active power losses. The optimal WT tap position, in regards to losses, has been evaluated using load flow simulations in Powerfactorys. The active power output has been recorded at PCC of both wind farms for a grid voltage and WT voltage equal to 1 pu and the losses have been calculated by subtracting the dispatched power with the power at PCC. The simulations have been conducted for dispatched active power between 0-100% and for all WT tap positions.
In general, the cases where the tap position increases the voltage in the collection grid, the current will be reduced. The initial hypothesis is therefore, that it is possible to reduce the losses using a WT tap position that will increase the voltage in the collection grid, hence, tap -1 and tap -2.

The results for the 33 kV and 66 kV wind farm are illustrated in figure 5.8 and figure 5.9, respectively.

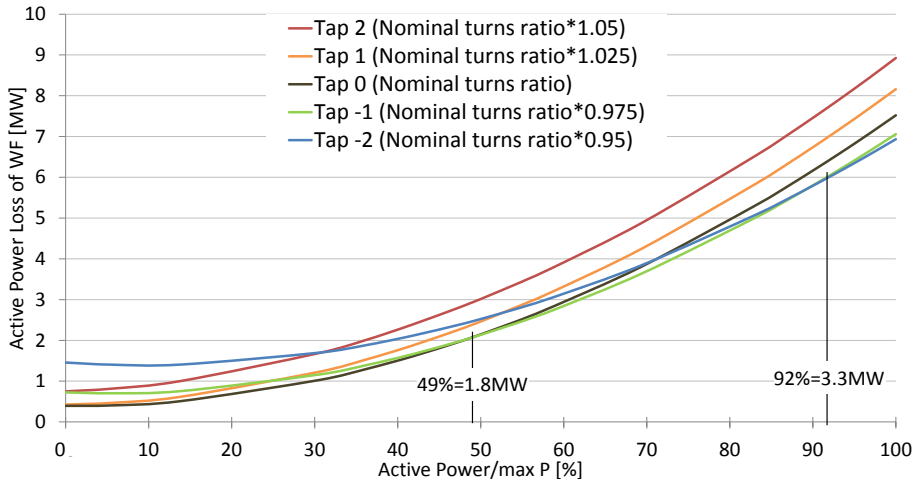

Figure 5.8: Active power losses at PCC for all tap positions of the WT transformers in relation to the dispatched power in the 33 kV WF.

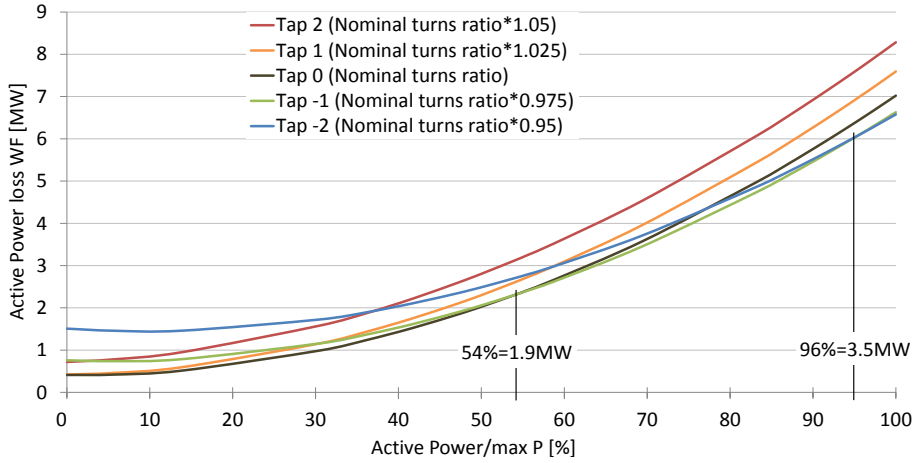

Figure 5.9: Active power losses at PCC for all tap positions of the WT transformers in relation to the dispatched power in the 66 kV WF.

At maximum power production the highest loss in both wind farms relates to tap position 2, hence, the highest turns ratio and lowest voltage on the HV side of the WT transformer. In general, for the same power transfer, a lower voltage leads to higher currents. As losses are proportional to the current squared, the losses will be higher for the biggest turns ratio of the wind turbines in the wind farms investigated, hence, for tap position 2. Thus, the loss curves, in figure 5.8 and 5.9, of tap positions 1 and 2, with lower voltage and higher current in the collection grid, are also steeper compared to the loss curves of the tap positions with higher voltage and lower current. The losses at high dispatched power therefore behave accordingly to the expectation of the initial hypothesis. However, figure 5.8 and 5.9 show that at low/zero dispatched power the losses are particular high for tap position -2, i.e. a high voltage and lower current in the collection grid. The reasons have been investigated through further load flow simulations. The simulations conducted showed that tap -1 and, particularly, tap -2 drive up the voltage in the sea-to-land cable and much higher losses occur at these tap positions in the sea-to-land cable. The connection between the voltage and the losses in the sea-to-land cable can be explained by where the losses in cables come from. Losses in cables can occur from the conductor, dielectrical material and sheath [41]. Dielectric losses also occur during no load [17]. As the dielectric losses depend on the voltage squared [2], it is assumed that the higher losses in the sea-to-land cable for WT tap positions that increases the voltage in the collection grid are caused by dielectric losses. This explains the behaviour of the graphs in figure 5.8 and 5.9. Hence, at lower dispatched power the losses are dominated by the dielectric losses in the sea-to-land cable whereas at higher dispatched power the losses are dominated by conductor losses.

The behaviour of the graphs in figure 5.8 and 5.9 leads to different optimal tap positions in terms of lowest losses for different dispatched power levels. As illustrated in figure 5.8, when the WT dispatched power P_{WT} for the 33 kV wind farm is below 1.75 MW the best tap position of the WT transformers is the neutral tap 0 in terms of losses. When P_{WT} is between 1.75 MW and 3.3 MW the optimal tap position = -1 (2.5% decrease in turns ratio) and at P_{WT} $>$ 3.3 MW the optimal tap position = -2 (5% decrease in turns ratio). Similar relationship, between the tap position and the losses at different dispatched power levels, are seen for the 66 kV wind farm. However, the dispatched power, for which tap position -1 and -2 leads to lower losses, is slightly higher compared to the 33 kV WF, as seen on figure 5.9. The difference between the wind farms is assumed to be caused by slightly flatter loss curves in the 66 kV WF compared to the 33 kV WF. As the taps on the WT transformers have the same dimensions in both wind farms, the increase in voltage, of for example 5%, measured in volts is higher for 66 kV compared to 33 kV, hence, the decrease in current will be equally higher. This results in flatter loss curves for the different tap positions in the 66 kV WF compared to 33 kV WF and the intersections of the curves in the 66 kV case therefore occur at higher power penetration.

The wind turbine transformers are equipped with De-Energized tap changers and the tap position is therefore rarely changed. Hence, the aim was to find the optimal tap position that would result on average lower active power losses over a long period of time, for example one year. A method to evaluate this, is using the capacity factor of a site. For example, if the two wind farms were erected at Hvide Sande with a capacity factor of 36% the associated average dispatched active power is 1.3 MW, hence, for both wind farms the optimal tap position is the neutral tap 0. If the wind farms are positioned at Horns Rev with $P_{CF,average} = 2112$ kW, using figure 5.8 and 5.9, the optimal tap position for both wind farms would be tap -1 in term of power losses. The investigation of the losses calculated over the range of the power curve for the tap position -1 at Horns Rev showed that the 33 kV wind farm has 2.9% lower losses using tap position -1 compared to the neutral position and the 66 kV wind farm has 1.8% lower losses. If the annual energy production of tap -1 and tap 0 is compared, the improvement using tap -1 is 0.1% for the 33 kV wind farm and 0.06% for the 66 kV wind farm. This improvement is very low and the difference is within the range for estimation uncertainties for predicting AEP [59]. It can therefore be argued, if it is worth using the taps on the wind turbine transformers to lower the losses.

The reactive power capabilities have been evaluated when the wind turbine transformers' tap position = -1. It is expected, that the reactive power capabilities will change for different tap positions, as the voltage controller on the wind turbines will try to compensate for the voltage difference in the turbine transformers caused by a tap change, by producing or absorbing reactive power. As example of the reactive power capabilities for WT tap -1, the situation with the worst reactive power capabilities has been chosen. Hence, the reactive power capabilities when the external grid is 0.9 pu is shown in figure 5.10.

Comparing figure 5.10 to figure 5.6, it is seen that the decreased turns ratio for tap -1 shifts the graphs to the right. For tap position -1, the WT transformer will try to lower the voltage on the LV side with 2.5% but the WT controller in PV mode is configured to control the voltage of the WT generator to a specific set point. Hence, to compensate for the this voltage difference the WTs shift their set point on their Q capability graph and produces more reactive power in order to increase the voltage. Therefore, the reactive power capability graphs for tap -1, in figure 5.10, are shifted to the right compared to tap 0, in figure 5.6. The opposite would happen if the taps on the WT transformer = 1, as the WT transformer would increase the LV set point and in order for the generator to compensate it would absorb more Q. This behaviour of the WTs when using the taps is also why tap changers sometimes are used to enhance the reactive power capabilities of wind power plants, as the tap position can change the operating point on the reactive power capability curve for wind turbines.

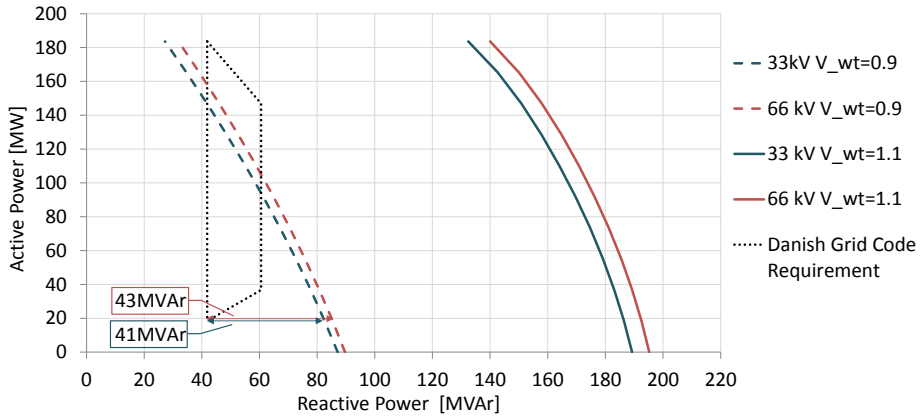

Figure 5.10: Reactive power capabilities recorded at PCC for the 33 kV and 66 kV wind farm when grid voltage is 0.9 pu and tap position at WT transformers is -1 = 2.5% decrease in nominal turns ratio.

For DETC, as the ones used on the WT transformers, the taps are fixed for a long period of time. For this type of tap changers, it would therefore, for example, be beneficial to operate the wind turbines at tap position -1 if the wind farm was located in an area where the grid almost always is depressed and therefore needs a large amount of Q production at PCC from the wind farm. However, for the cases in this thesis, the enhanced Q production for tap -1 leads to an even higher Q-compensation need at PCC in order to fulfil the Danish grid code requirements. As illustrated in figure 5.10, the additional inductive Q-compensation needed for the 33 kV and the 66 kV wind farm is 41 MVAr and 43 MVAr, respectively. This is 28 MVAr more compared to the results obtained in section 5.2, where the wind turbines transformers were in neutral position. The additional reactive power that needs to be compensated would increase the cost of the device used as reactive power compensation. In order to fully evaluate if tap position -1 benefits the operation of the wind farms, the cost benefits of the active losses and the cost loss of the additional reactive power compensation have been compared. This evaluation is carried out in section 5.5.

It has briefly been investigated, using load flow simulations in Powerfactory, if the use of taps on the substation transformers could lower the additional Q-compensation needed when the WT transformers' tap position = -1. The investigation revealed that if the turns ratio of the substations transformers were increased (tap $<$ 11), the wind farms were able to absorb more reactive power but on the expensive of the active power flow where losses would increase. Therefore, using this configuration has not been investigated any further.

5.4 Fault Analysis

The results of the fault current in different fault cases are evaluated in this section. The peak short circuit current has been obtained at three different locations in the wind farm network. The fault current can be used to evaluate the switchgear requirements. As the voltage is doubled in the 66 kV WF compared to the 33 kV WF, the initial hypothesis is that the fault current will be lower in the 66 kV wind farm. The hypothesis is evaluating for the following faults:

- Balanced three phase fault
- Line to line fault
- Double line to ground fault
- Single line to ground fault

The three fault locations chosen to evaluate the peak short circuit current are at the high voltage busbar at PCC, the busbar at the LV side of the substation transformer A and the busbar at the HV side of the transformer connected to wind turbine AA01, which is located as the last wind turbine in an array furthest away from substation A. The maximum short circuit current has been evaluated in Powerfactory using the IEC 60909 method.
The peak short circuit current for a three phase fault in the three fault locations is shown in figure 5.11. The line to line fault and the double line to ground fault gave similar results.

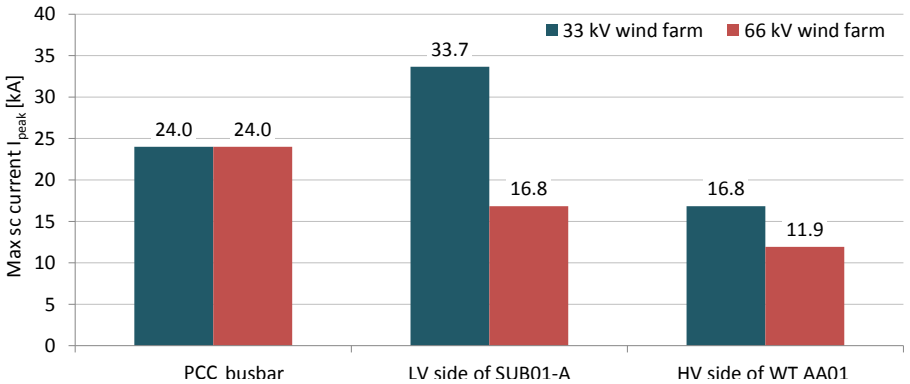

Figure 5.11: Fault current for a three phase short circuit fault in three different fault locations.

The results in figure 5.11 show, that for two of the locations the fault current is significantly lower in the 66 kV case compared to the 33 kV case. The differences between the two wind farms can best be explained by considering the differences and similarities of the components in the wind farms.

The fault current is the same in both cases at the HV busbar at PCC as the parameters of the components used in the 33 kV and 66 kV wind farm are the same from the high voltage side of the two substation transformer to PCC.

The fault current at the LV side of substation transformer A is doubled in the 33 kV case compared to the 66 kV case. The fault current in this location depends on the impedance of the substation transformer. The impedance of the transformer can be evaluated using equation 5.4. As the resistance in equation 5.5 is very small, the impedance of the transformer is dominated by the reactance X in equation 5.6. Hence, as the voltage level on the LV side of the transformer increases with a factor 2 from the 33 kV wind farm to the 66 kV wind farm, the impedance will increase with a factor 4.

$$Z = \sqrt{R^2 + X^2} \tag{5.4}$$

$$R = \frac{U^2}{S} * R_{percentage} \tag{5.5}$$

$$X = \frac{U^2}{S} * X_{percentage} \tag{5.6}$$

The current can be evaluated using equation 5.7. Therefore, if the voltage increases with a factor 2 and the impedance increases with a factor 4, the fault current in the 66 kV WF should be half the size of the fault current for the 33 kV WF, when a fault occurs at the busbar of the LV side of substation transformer A. The results in figure 5.11 are consistent with the analytical evaluation.

$$I = \frac{U}{Z} \tag{5.7}$$

In the fault location at the busbar on the HV side of the wind turbine AA01 transformer, the fault current in the 66 kV case is 71% of the fault current in the 33 kV case. Hence, the fault current is not halved comparing the two cases in this location. To understand why, a similar evaluation of the impedances have been carried out. Due to the location of the fault, the fault impedance, compared between the 33 kV and 66 kV wind farm, will depend on the impedance of the substation transformer, the impedance of the cables in the array which connects turbine AA01 to the substation busbar and the impedance of the sea-to-land cable. This is best illustrated by a drawing, see figure 5.12.

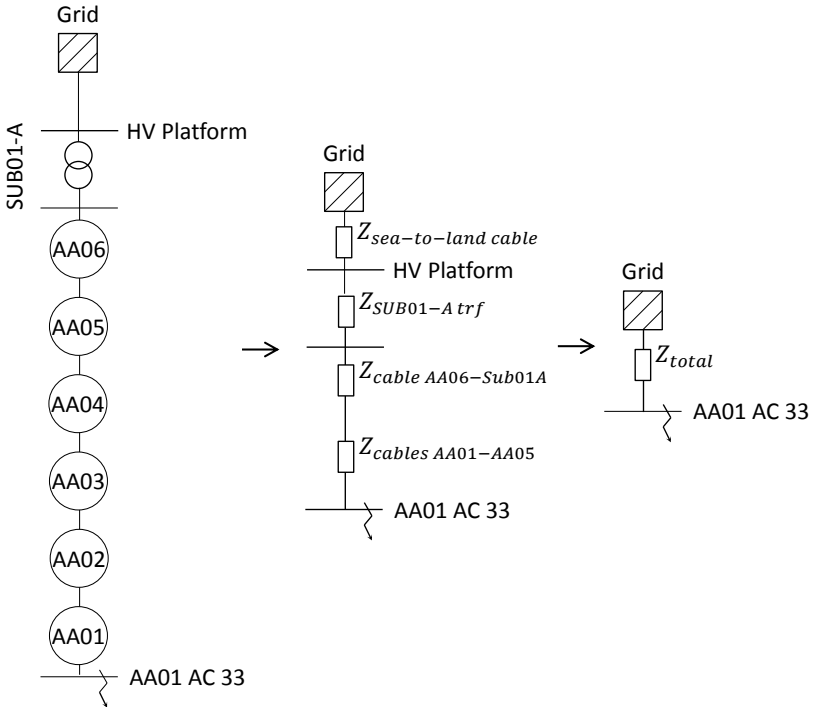

Figure 5.12: Impedance for fault location at the HV side of WT AA01 transformer.

The impedance of the cable array connecting wind turbine AA01 to the substation transformer has been split into $Z_{AA06-Sub01A}$ and $Z_{AA01-AA05}$, as a larger cable with a different impedance between WT AA06 and the substation is used in the 33 kV wind farm compared to the cables connecting wind turbine 1, 2, 3, 4 and 5. For the 66 kV wind farm the same type of cable is used in the full array.

The impedance of the cables is found from the cable's positive sequence resistance and reactance, as defined in Powerfactory, using equation 5.4. As the resistance and reactance of the cables are given in Ohm/km, the cable length is taken into consideration when evaluating the impedance. The parameters of the cables are captured in table 4.5 and 4.6 in chapter 4. Hence, the impedance of the cable array is expressed in equation 5.8 for the 33 kV case and in equation 5.9 for the 66 kV case.

$$\begin{aligned} Z_{33} &= \sqrt{R^2_{cable\,A} + X^2_{cable\,A}} \; * l_{cable\,AA01-AA05} \\ &\quad + \sqrt{R^2_{cable\,B} + X^2_{cable\,B}} \; * l_{cable\,AA06-Sub01A} \\ &= 0.944\ \Omega \end{aligned} \tag{5.8}$$

$$\begin{aligned} Z_{66} &= \sqrt{R^2_{cable\,A} + X^2_{cable\,A}} \; * l_{cable\,AA01-AA06} \\ &= 1.502\ \Omega \end{aligned} \tag{5.9}$$

The impedance of the substation transformer for the 33 kV wind farm, calculated using equation 5.4, is 0.635 Ω and for the 66 kV wind farm it is 2.54 Ω, hence, a factor 4 larger. The sea-to-land cable from the substation transformer to the grid connection should also be taken into account. As it is the same cable that is used in the 33 kV wind farm and the 66 kV wind farm, the impedance and the length of the cable is the same. Using the parameters of the cable in table 4.5 in section 4.2, the impedance of the sea-to-land cable can be calculated according to equation 5.4. To get the result in Ohm, the result is multiplied with the length of the cable. However, due to the location of the fault the impedance of the sea-to-land cable should be referred to the primary side (LV side) of the substations transformer, as expressed in equation 5.10. Hence, the impedance of the sea-to-land cable referred to the primary side for the 33 kV wind farm is 0.31 Ω and 1.2 Ω for the 66 kV wind farm.

$$Z'_{cable} = \alpha_t^2 * Z_{sea-to-land\ cable} \tag{5.10}$$

The total impedance is then the sum of the cable array, the substation transformer and the sea-to-land cable. For the 33 kV case the impedance is therefore 1.9 Ω and for the 66 kV case it is 5.3 Ω. Comparing the two results, the increase in impedance going from the 33 kV to 66 kV is therefore $5.3/1.9 = 2.8$. As the voltage increases with a factor 2, the current in the 66 kV wind farm should then be $2/2.8 = 72\%$ of the current in 33 kV wind farm. According to the results obtained in Powerfactory the fault current using 66 kV is 71% of the current obtained using 33 kV. The slight different in the theoretical evaluation and the results obtained in Powerfactory could be explained by the actual voltage level when running the simulation in Powerfactory, as it deviates slightly from the theoretical value of either 33 kV or 66 kV.

Similar relationships of the three phase fault current between the 33 kV and the 66 kV wind farm in the three fault locations are obtained for the line to line fault and the double line to ground fault.

However, for the single line to ground fault the results were different in two of the locations, as illustrated in figure 5.13. For both wind farms the fault current is significantly lower compared to the other faults analysed. This can be explained by the configuration of the substation transformers and the wind turbine transformers. The substation transformers are Δ-connected on the LV side and Y-connected on the HV side. The wind turbine transformers are Y-connected on the LV side and Δ-connected on the HV side. As the fault locations investigated are either on the LV side of the substation transformer or the HV side of the wind turbine transformer, due to the delta connections, no zero current should be able to flow as the transformers are not grounded on the side using delta connection. According to this reasoning, there should not be a fault current at all for a single line to ground fault.

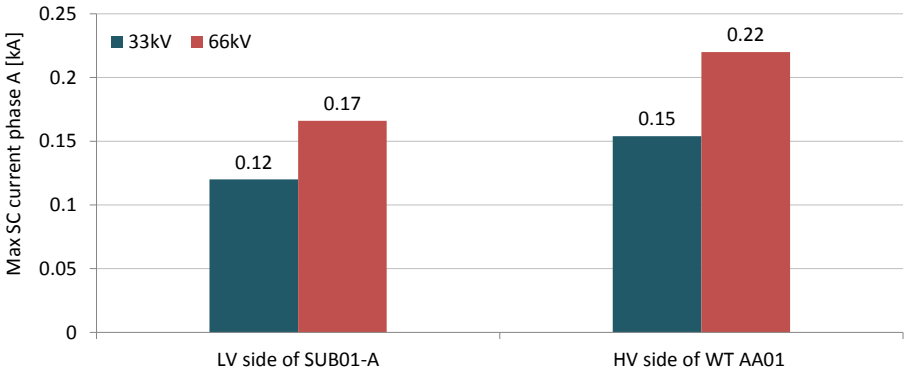

Figure 5.13: Fault current at single line to ground fault.

The reason for the small fault current for the single line to ground faults, illustrated in figure 5.13, is due to the line capacitance of the cables, which make the connection to ground. This has been verified by setting the zero sequence capacitance $\approx 0\ \Omega$/km for the cables in the Powerfactory models. The following short circuit simulations conducted showed a fault current ≈ 0 A. In the wind farms investigated, the capacitance of the cables is lower in the 66 kV WF compared to the 33 kV WF, leading to a higher impedance. However, the impedance related to the cable capacitance increases with less than a factor 2 going from the 33 kV wind farm to the 66 kV wind farm. As the voltage level increases with a factor 2, the fault current for the single line to ground fault is slightly higher in the 66 kV wind farm.

Overall, the fault analysis confirmed the initial hypothesis and showed that using 66 kV instead of 33 kV will significantly lower the fault current in all fault cases except the single line to ground fault. Hence, the lower fault current in the 66 kV case leads to lower switchgear requirements compared to the 33 kV case.

5.5 Economic Analysis

The economics of the wind farms have been evaluated at the basis of the technical analysis. The economic analysis includes an evaluation of the installation cost of those components with different properties in the 33 kV wind farm compared to the 66 kV wind farm, according to the design and technical requirements of each wind farms. Hence, the cost of the cables, transformers, switchgear and reactive power compensation have been evaluated. In this pre-feasibility study, it has not been possible to obtain specific prices for these components from manufacturers. Instead, the cost of components are evaluated using cost expressions, which associate the cost with the rating of certain parameters of the components. The cost of the active power losses are also evaluated. Furthermore, changes in installation cost and AEP when using 66 kV instead of 33 kV are estimated and the results are used to evaluate the cost of energy for both wind farms in relation to each other.

Cost expressions

Cost expressions are a very simplified method used to estimate the cost of wind farm components and it is therefore important to be critical of the economic results obtained by using cost expressions. The cost models presented in this section are developed by [52], where the cost expressions are based on information gathered by various sources. Other literature, such as [49] [53] [25], assessing the cost of wind farms also base their investigation on [52]. Hence, the cost models are assumed to provide a good estimation of the economics of wind farms.

The cost of cables are expressed by equation 5.11 [52]. The cable cost expression is based on cost information considering the conductor area and rated voltage. Therefore, the parameters A_{cable}, B_{cable} and C_{cable} are dependent on the voltage level. Their values for 33 kV, 66 kV and 132 kV can be found in appendix A.2. The cost of the cables also depends on the rated power of the cable S. S is defined by equation 5.12 where U_{rated} is the voltage of the cable and I_{rated} is the current of the cable. In the collection grid of both wind farms two different cables are used with different current rating. Hence, the calculations are carried out for both cables in the two wind farms and the overall collection grid cable cost is found for each wind farm taken the lengths of the cables into account.
The cable cost expression increase exponentially with the rated power. For the same rated power, if calculating the cost using the cable cost parameters associated with 33 kV and 66 kV, the cost of the cables is higher in the 33 kV case.

The parameters are based on information regarding the cross section area and voltage level. Hence, the cable cost expression does to some extend consider that less material is used in a 66 kV cable leading to lower cost compared to a 33 kV cable of the same rated power.

$$C_{cable} = A_{cable} + B_{cable} * exp\,(C_{cable} * S) \tag{5.11}$$

$$S = \sqrt{3} U_{rated} I_{rated} \qquad [VA] \tag{5.12}$$

The cost of the transformers (trf) is expressed by equation 5.13 [52]. According to the expession the cost depends on the rated power of the transformer P_{rated}. The transformer cost paramaters can be found in appendix A.2. According the equation 5.13, the transformers in the 33 kV wind farm will cost the same as the transformers in the 66 KV wind farms as the cost is defined by the power rating of the transformers. However, according to [66] the estimated increase in wind turbine transformers is around 20-30% when moving to higher voltages. Therefore, in the cost calculations of the wind turbine transformers an increase of 25% have been used. Potential increase or decrease in the cost for the substation transformers is unknown and therefore not accounted for.

$$C_{trf} = A_{trf} + B_{trf} * P_{rated}^{\beta_{trf}} \tag{5.13}$$

The cost of switchgear (SG) is expressed by equation 5.14 [52]. The cost parameters can be found in appendix A.2. The expression gives a linear relation of the cost dependant on the switchgear's rated voltage U_{rated}. According to equation 5.14, the cost of the switchgear does not depend on the short circuit current that the switchgear must be able to handle. It is mentioned in [68] that lower short circuit requirements, as seen the 66 kV case, would reduce the cost. However, the size of the cost reduction is unknown and is therefore not accounted for. There is therefore a high uncertainty on whether the switchgear cost expression provides with good estimates of the cost of switchgear in the two wind farm cases.

$$C_{SG} = A_{SG} + B_{SG} * U_{rated} \tag{5.14}$$

The additional inductive reactive power compensation needed in both wind farms are implemented using a shunt reactor. The cost expression for the shunt reactor is expressed in equation 5.15 [52]. According to the equation, the shunt reactor cost is $2/3$ of the transformer cost of same rating.

$$C_{shunt\ reactor} = \frac{2}{3} C_{trf} \tag{5.15}$$

Energy losses shall be evaluated for the entire life time of the wind farms. The lifetime of wind farms is set to 20 years [47] [73]. In Denmark, support is given to wind farm operators. According to the *Danish Ministry of Climate, Energy and Building*, Danish offshore wind farms receive between 0.519 - 1.051 DKK/kWh for about 12.5 years [26]. In these calculations, a support of 0.979 DKK/kWh = 131 €/MWh is used, which is equivalent to the expected settlement price for Kriegers Flak [26]. For the remaining 7.5 years, the average spot price for Western Denmark DK1, where Horns Rev is located, is used as the electricity price. As the future electricity price is unknown, although often researched, the average spot price in 2014 for DK1 equal to 229DKK/MWh = 31 €/MWh is used [70]. Hence, the cost of energy losses for the lifetime of the wind farms are calculated by equation 5.16. A similar equation can be used to estimate the profit of a wind farm. When using this simplified cost expression for the losses, it is important to note, that it does not take potential developments of prices and support into account.

$$\begin{aligned} C_{losses} = E_{loss}^{peryear} * 12.5\text{years} * 131\frac{€}{\text{MWh}} \\ + E_{loss}^{peryear} * 7.5\text{years} * 31\frac{€}{\text{MWh}} \end{aligned} \tag{5.16}$$

For this thesis, the cost variations caused by voltage differences is interesting to consider. The development of an overall relationship between cost and voltage is out of scope for this thesis, however, a tendency can be seen by considering the cost expressions dependant on the voltage in this section. The cost of switchgear is linearly proportional to the voltage, the cost of cables is implicit related to the voltage through voltage specific parameters and the cost of losses is proportional to $1/U^2$ for systems of same power rating. If these cost impressions are considered in combination with each other, the overall cost, as a function of the voltage, is therefore assumed to include a minimum. At minimum, the lowest possible cost is obtained for a specific voltage level. How steep or flat the cost will increase on either side of the minimum is unknown. It is also unknown where the two cases considered in this thesis are located on such a voltage-cost graph and whether either 33 kV or 66 kV actually represents the minimum cost possible.

Results

In the technical evaluation of using tap changers in the WT transformers the results showed that tap position -1, i.e. a decrease in turns ratio, would lead to lower losses and an additional need of inductive reactive power compensation in both wind farms when compared to the neutral tap position. Evaluating this in

an economic view, the improvement in the losses can be interpreted as a profit while the additional reactive power compensation needed is an added cost.

The additional inductive reactive power compensation needed in both wind farms is 28 MVAr which is estimated to cost €0.37M, using equation 5.15. The improvement in losses for the 33 kV and the 66 kV wind farm, comparing the neutral tap position to tap position -1, is 20 GWh and 11 GWh, respectively, for the entire lifetime. This improvement leads to an additional profit for tap position -1 estimated to be €1.9M for the 33 kV wind farm and €1.1M for the 66 kV wind farm, using equation 5.16. Combining the cost of the additional reactive power compensation with the profit of the reduction in losses, the total economic benefit, if operating the wind farms for the entire life time at tap position -1 compared to the neutral position, is an additional profit of €1.5M for the 33 kV wind farm and €0.7M for the 66 kV wind farm.
With the focus of this thesis, the important thing to take from this investigation, is that the economic benefits of using WT tap changers in the 66 kV wind farm is less than half of the economic benefits in the 33 kV wind farm.

The overall economic comparison between the 33 kV and the 66 kV wind farm has been based upon the technical performance of the wind farms when the taps of the transformers are in neutral position. Technical results, used to evaluate the costs, are based on Powerfactory simulations conducted for the whole range of the power curve and analysed using the Weibull distribution at Horns Rev. The economic results for the 33 kV wind farm and 66 kV wind farm are captured in table 5.1 and 5.2, respectively.

In the hypothesis mentioned in the introduction, it was initially thought, that using higher voltages would cause an increase in the cost of components and a decrease in the cost of energy losses in the 66 kV case. This is also the result when comparing the two cases. However, the difference in cost between the two wind farms is very small. Whether the correct prices of the components have been calculated is highly uncertain. For example, is the cost of the substation transformer considered to be the same in both cases, however, in reality it is more likely that the cost of the 66 kV transformer is highest. The cable cost expression is based on information regarding the conductor area and the voltage level. This is also shown on the cost of the collection grid cables, as the results give a higher cost in the 33 kV case. It is therefore assumed, that the cable cost expression does consider lower a amount of copper material used in the 66 kV case.

The costs of the two wind farms presented in table 5.1 and 5.2 have been used to estimate differences in the cost of energy between the two cases.

Table 5.1: Costs of the 33 kV wind farm.

Description	Specification	Cost [M €]
Turbine switchgear	51 x 33 kV	2.9
Turbine transformer	51 x 4 MVA	4.0
Cables collection grid	45.7km 33 kV	11
HV cable to PCC	47.8km 132 kV	33
Substation transformer	2 x 180 MVA	2.1
Substation MV switchgear	2 x 33 kV	0.11
Reactive power compensation	13 MVAr	0.23
Total collection grid cost		**53**
Energy losses (life time)	678 GWh	63
Total cost ($C_{components} + E_{losses}$)		**116**

Table 5.2: Costs of the 66 kV wind farm.

Description	Specification	Cost [M €]
Turbine switchgear	51 x 66 kV	4.0
Turbine transformer	51 x 4 MVA	5.0
Cables collection grid	45.7km 66 kV	9.9
HV cable to PCC	47.8km 132 kV	33
Substation transformer	2 x 180 MVA	2.1
Substation MV switchgear	2 x 66 kV	0.16
Reactive power compensation	15 MVAr	0.25
Total collection grid cost		**54**
Energy losses (life time)	636 GWh	59
Total cost ($C_{components} + E_{losses}$)		**114**

Levelised Cost of Energy

A complete feasibility study used to calculate the levelised cost of energy of the two wind farms is a very extensive procedure and therefore out of scope for this thesis. Instead, the LCOE for the 33 KV wind farm has been based upon the average cost of energy for offshore wind farms of similar sizes found in literature. As mentioned in section 2.3 and expressed in equation 2.6, LCOE depends on the annual energy production and the installed capital cost. Therefore, by comparing the increase or decrease in ICC and AEP when using 66 kV instead of 33 kV, it is possible to estimate the LCOE of the 66 kV wind farm relatively to the 33 KV wind farm.

The LCOE of offshore wind power plants according to the literature is 210 USD/MWh [8], 225 USD/MWh [71] and 180 €/MWh [56]. Using these figures as references, the LCOE of the 33 kV wind farm has been set to be 190 €/MWh. As the LCOE can be calculated according to equation 2.6 in section 2.3, the LCOE for the 66 kV wind farm relative to the 33 kV wind farm can be expressed by equation 5.17. Here α_{ICC} is the estimated increase or decrease in percentage of the installed capital cost and β_{AEP} is the estimated percentage increase in AEP moving from 33 kV to 66 kV.

As $\frac{AEO}{AEP_{net}}$ is small, equation 5.17 can be simplified to equation 5.18 where the LCOE for the 66 kV wind farm is expressed as a function of the LCOE of the 33 kV wind farm.

$$LCOE_{66} = \frac{(ICC * \alpha_{ICC}) * FCR + AEO}{AEP_{net} * \beta_{AEP}} \tag{5.17}$$

$$LCOE_{66} \approx \frac{\alpha_{ICC}}{\beta_{AEP}} LCOE_{33} \tag{5.18}$$

The annual energy production of both wind farms, calculated using the power curve and the Weibull distribution at Horns Rev, is captured in table 5.3. The AEP is calculated using the efficiency of the wind farms when the efficiency is obtained considering wind speeds between 0-25m/s. This means, that losses below cut in wind speeds when the turbines are not producing power are also included. This will of course lower the efficiency slightly compared to the efficiency that could be obtained if only the losses associated with wind speed between cut-in and cut-out wind speeds were taken into account. From the obtained AEP of both wind farms, it is calculated that the AEP increases with $\beta_{AEP} = 0.23\%$ moving from 33 kV to 66 kV.

Table 5.3: AEP of the 33 kV wind farm and the 66 kV wind farm.

	33 kV Wind Farm	**66 kV Wind Farm**
Efficiency [%]	96.4	96.6
AEP [GWh]	910	912

The installation cost of the components, which according to the design and technical performance of the 33 KV and 66 kV wind farms will be different, was captured for the two cases in table 5.1 and 5.2, respectively.

In general, the installed capital cost of wind power plants can be broken down into the cost of wind turbines, electrical infrastructure/grid connection, foundations and planning & installation [69] [56]. The biggest share of the installed capital cost is the wind turbines of around 70% [69] [60]. The cost of the components calculated in this thesis, referred to as collection grid cost, fall into the category of electrical infrastructure, apart from the turbine switchgear and transformer which is in the wind turbine category. The installed capital cost of offshore wind power plants, according to the literature, varies between 3300-5000USD/kW [69] and 2500-6500 USD/kW [71]. Using these costs as references, the installed capital cost for the 33 kV wind farm has been set to 3.9M €/MW. Hence, the total installation cost of the 33 kV wind farm is assumed to be €716M. The collection grid cost of the 33 kV wind farm equal to €53M and of the 66 kV wind farm it is equal to €54M, see table 5.1. The increase in the collection grid cost is therefore 2.3% when moving from 33 kV to 66 kV. As the collection grid cost is 7.4% of the total estimated installation cost in the 33 kV wind farm, the overall investment cost ICC increases with $\alpha_{ICC} = 0.18\%$ in the 66 kV wind farm compared to the 33 kV wind farm.

Both the increase in installed capital cost and the increase in AEP, when comparing the 66 kV wind farm to the 33 kV wind farm, are very close to 0.2%, which is relatively low. Calculating the $LCOE_{66}$ using the expression in 5.18, the LCOE of the 66 kV wind farm is the same as the LCOE of the 33 kV wind farm. From the economic assessment, it is therefore not possible to conclude any changes in LCOE for the 66 kV wind farm when compared to the 33 kV wind farm.

5.6 Comparison and Discussion

Table 5.4 provides a summary of the main results in terms of design parameters, technical performance and economic estimations of the 33 kV wind farm and the 66 kV wind farm.

Table 5.4: Summary and comparison of results between the two wind farms.

	33 kV Wind Farm	*66 kV Wind Farm*
Design Parameters		
Collection grid voltage	33 kV	66 kV
Collection grid cables	150mm^2 396A 0.14$\frac{\Omega}{\text{km}}$ 500mm^2 716A 0.06$\frac{\Omega}{\text{km}}$	95mm^2 300A 0.23$\frac{\Omega}{\text{km}}$ 150mm^2 375A 0.146$\frac{\Omega}{\text{km}}$
WT transformer	$\alpha_t = 0.69/33$	$\alpha_t = 0.69/66$
Substation transformer	$\alpha_t = 33/132$	$\alpha_t = 66/132$
Technical Performance		
Net AEP	910 GWh	912 GWh
Efficiency	96.4%	96.6%
WF yearly energy loss	34 GWh	32 GWh
Collection grid cables yearly energy loss	3.7 GWh	1.8 GWh
Inductive Q-compensation	13 MVAr	15 MVAr
Max. SC current 3-ϕ fault	34 kA	17 kA
Loss reduction for tap -1 compared to neutral tap	2.9%	1.8%
Inductive Q-compensation tap -1	41 MVAr	43 MVAr
Economic Estimation		
Increase in profit for tap -1 compared to neutral tap (life time)	€1.5M	€0.7M
Collection grid cost	€53M	€54M
Cost of energy losses (life time)	€63M	€59M
LCOE (estimated relatively to each other)	190 €/MWh	190 €/MWh

Discussion of technical and economic results

As shown in table 5.4, using 66 kV instead of 33 kV resulted in a very small increase in efficiency. Although the losses in the collection grid cables are reduced with around 50% in the 66 kV wind farm compared to the 33 kV wind farm, due to the fact that the losses in the collection grid cables are only a very low share of the total losses in the wind farms, the overall reduction of losses is only 6% lower when using 66 kV instead of 33 kV. The low loss reduction also resulted in a relatively low increase in the annual energy production of 2 GWh = 0.2% more per year in the 66 kV case compared to the 33 kV case.

Neither of the two wind farms investigated were able to fulfil the Danish grid code requirements from Energinet.dk in terms of reactive power capabilities, when only the wind turbines' reactive power capability was used. The large production of Q from particularly the sea-to-land cable resulted in a need for inductive reactive power compensation in both cases. The analysis of the load flow simulation results of the 33 kV wind farm showed that an inductive reactive power compensation of 13 MVAr was needed at PCC in order to fulfil the Danish grid code requirements. The 66 kV wind farm needed 15 MVAr inductive reactive power compensation at PCC. The increase in Q-compensation needed for the 66 kV wind farm is assumed to be caused by an enhanced production of reactive power in the collection grid cables due to the higher voltage in the collection grid in the 66 kV wind farm compared to the 33 kV wind farm. This was verified through extended load flow simulations. A shunt reactor can be implemented in both cases to compensate for the remaining inductive reactive power needed. The shunt reactor increases the losses in the wind farm slightly as it uses 37 kW in the 66 kV wind farm and 33 kW in the 33 kV wind farm. However, this added loss is almost the same in both cases and the loss comparison therefore gives a similar result with and without the shunt reactor.

The biggest impact on using 66 kV rather than 33 kV was seen on the fault current levels at different fault cases. For a fault located on the LV side of substation transformer A, the fault current in the 66 kV wind farm was half the size of the fault current in the 33 kV wind farm for all fault cases except the single line to ground fault. For the same fault cases except the single line to ground fault, if a fault was located on the HV side of the WT AA01 transformer, placed at the far end of an array, the fault current was also much larger in the 33 kV case compared to the 66 kV case. However, the difference in fault current at this location was lower due to the higher impedance of the array cables in the 66 kV case. For a single line to ground fault, at the above mentioned locations, the fault current was very low due to delta-configuration on the transformer side at which the faults were located.

As an additional study the use of tap changers on the wind turbine transformers was conducted. The investigation showed that the optimal tap position of the WT transformers in terms of active power losses changes dependent on the dispatch active power level, hence, on the wind speed. At smaller wind speeds the best tap position was the neutral tap and at medium to high wind speeds the best tap position was tap -1, i.e. a decrease in turns ratio causing higher HV level of the WT transformers, and at very high wind speeds the optimal tap = -2 which further decreases the turns ratio. Both wind farms showed this pattern. It is assumed that the reason for this relationship between the tap change position and the dispatched active power are caused by the conductor losses dominating at high power levels and the dielectric losses dominating at low power levels. Tap position 2 and 1 leads to lower voltage on the HV side of the WT transformer, hence, increasing the current in the collection grid. As the conductor losses increase with current squared and the current increases with increased power, the conductor losses at tap 2 and 1 will be higher at particularly higher power levels. At lower power levels the dielectric losses in the sea-to-land play a significant role for tap position -2 and -1, as the voltage is higher in these cases. This was verified through extended load flow simulations. For tap position -1, the overall losses compared to the neutral tap was improved with 2.9% in the 33 kV WF and 1.8% in the 66 kV WF. However, the same tap position increases the reactive power compensation needed in both cases with 28 MVAr, as the WT generators try to compensate for the voltage different caused by the change in tap position by producing more Q. The technical performance of the wind farms in tap position -1 was transferred into economic estimations. The analysis showed a small increase in profit which was slightly lower for the 66 kV case compared to the 33 kV case.

Disregarding the use of taps on the WT transformers, the economic evaluation of both wind farms gave very similar results. The installation cost would increase slightly in the 66 kV wind farm caused by higher cost of switchgear due to the higher voltage level, an increased cost of the shunt reactor due to the increase reactive power compensation needed and an estimated increased cost of the WT transformers. However, the component cost estimations are very uncertain which could be a cause of the low cost difference between the two cases. The lower losses in the 66 kV case leads to a small increase in AEP compared to the 33 kV case. As the economic differences are small and as the increase in installation cost contradicts the increase in AEP, no difference in the cost of energy of the two wind farms was noted when estimated relatively to each other.

Overall, the only big difference in the technical and economic comparison between the two wind farms was seen on the fault current. Unless the fault current causes a problem in generic 33 kV wind farms, according to the investigation carried out in this thesis, it can not be concluded that it is more beneficial to use either 33 kV or 66 kV in the collection grid.

Thesis results in a broader perspective

As mentioned in the introduction a limited amount of published literature investigates if using higher voltages in the collection grid would benefit the technical performance and the economics of wind farms. The articles published on this topic have similar conclusions to the results obtained in this thesis in terms of lower fault current and lower losses when using higher voltages in the collection grid.

In this thesis, the reduction in energy losses does not improve significantly when using 66 kV in the collection grid instead of 33 kV. The choice of wind turbines and the size of the wind farm are likely to be important factors in the evaluation of losses. If a larger wind turbine was implemented, for example a 7 MW rather than a 3.6 MW, the current on the cables will increase which results in higher losses on the cables. If 66 kV are used instead of 33 kV then the reduction in losses, comparing the two cases, will be higher for higher power levels. Hence, the benefit of using higher voltages increase with an increasing size of wind turbines. Article [68], which also evaluated the losses when using higher voltages in the collection grid of wind farms, supports this assumption. The investigation in the article is based on 5 MW wind turbines and the total size of the wind farm is 1005 MW. In their loss investigation the loss reduction is larger compared to the results obtained in this thesis.

The reduction of losses could also be increased if the resistance of the cables in the 66 kV WF was lower and closer to the resistance of the cables in the 33 kV WF. The losses in the collection grid cables in the 66 kV WF can minimum be 1/4 of the losses in the 33 kV WF, as the voltage is doubled, hence, for the same power the current will be halved and the losses 1/4 of the losses in the 33 kV case. However, the higher resistance caused by the lower cross sectional area of the cables used in the 66 kV case, results in less reduction of losses when the two cases are compared. To avoid a higher cable resistance in the 66 kV case, cables with the same cross sectional area in both wind farms could be used. However, one of the benefits of using a lower cross sectional area for the cables in the 66 kV wind farm is the lower amount of copper used which will decrease the cost of the cables. There is therefore a trade-off between reducing losses in the cables and reducing the cable size. Hence, it is likely that the optimal size of the cables is found by considering both.

In the investigation carried out in this thesis the economic benefits were unnoticeable when using higher voltages in the collection grid. However, the literature published on the topic estimates some economic benefits mainly caused by the option of eliminating the offshore substation transformer when using higher voltages in the collection grid. The effect of removing the substation transformers

could, according to [49], result in a 2.4% lower investment cost. However, the set up of the wind farms investigated in [49], originally included a 33/132 kV offshore substation transformer and an 132/450 kV onshore transformer, where for the higher voltage option the offshore substation would be removed and the onshore substation would directly convert the collection grid voltage into 450 kV. In the set up of the wind farms considered in this thesis the connection to the grid is at the 132 kV voltage level, hence, in either wind farm cases a transformer converting the collection grid voltage to 132 kV is necessary. Having the transformer on land could possibly reduce the cost of the transformer compared to a similar transformer installed offshore. However, if a voltage level of 66 kV was used for the sea-to-land cable due to a higher current in the cable the losses would increase and the extra cost of losses might even out the added economic benefit of leaving the transformer on land. It is therefore assumed that for the wind farms investigated in this thesis the elimination of the substation transformers is not an option and moving the substation transformers in the 66 kV wind farm to land would most likely not lead to any significant economic benefits.

The results of the investigation of the reactive power capabilities in this thesis seem to contradict the results of similar investigations carried out by [68] [65]. Where the conclusion in this thesis is a slight increase in the needed reactive power compensation for the 66 kV wind farm compared to the 33 kV wind farm, the literature published on the topic mention a decrease in the reactive power compensation needed for wind farms of higher voltages. It is, however, difficult to compare the cases as the layouts of the wind farms are different and the reactive power capabilities are tested under different conditions. With this in mind, analysing the results in [65] a possible explanation of the different conclusions can be found.

The wind farms investigated for the reactive power capabilities in [65] are 90 MW and the results are compared against the UK grid code. According to their investigation, the most strenuous requirements is to provide a 0.95 lagging power when exporting maximum power. In other words, the wind farms in [65] needs capacitive Q-compensation at high dispatched active power levels. As wind farms of higher voltages are able to produce more Q, because the production of Q in the cables increase with increased voltage, the capacitive Q-compensation needed is lower in the wind farms of higher voltages in [65]. If these results are seen in relation to the two wind farms investigated in this thesis, it is assumed that the different Q-compensation conclusions are caused by the different sizes of the wind farms investigated and the comparison to different grid codes. The size of the wind farms in this thesis are larger and the length of the sea-to-land cable is longer compared to the wind farms in [65]. This leads to a higher reactive power production from the collection grid cables and particularly from the sea-to-land cable for the two wind farms. Hence, there is no lack of reactive power

production in the cases in this thesis and the large production of Q actually leads to the need of inductive Q-compensation instead. The cases in this thesis are also compared against the Danish grid code and not the UK grid code. The Danish grid codes for Q-requirement lower the requirements for reactive power production of wind farms at higher dispatched active power level whereas the UK grid code has the same capacitive Q-requirements for all dispatched active power levels. It is therefore likely, that the capacitive reactive power compensation needed at maximum export of power in [65] would be lower if the reactive power flow was compared against the Danish grid code.

Comparing the results of the thesis with the available literature shows that the layout and design of wind power plants and the choice of scenarios used to investigate and analysis the technical performance and the economics of the wind farms are important factors in determining which voltage level is better to use in the collection grid of wind farms. This is important to keep in mind when attempting to make an overall conclusion and especially if the results of the investigation are taken a step further and used for wind power plant developers in their choice of voltage level in the collection grid.

Chapter 6

Conclusion and Future Work

The aim of this thesis has been to investigate if using higher voltages in the collection grid of wind power plants could lead to improved technical performance and economic benefits of wind farms. The thesis contributes to the interests of the wind power industry today, where solutions that will lower the cost of energy without compromising the technical performance of wind power plants are highly sought for. The focus of this thesis has been on *"Wind power plants internal distribution system and grid connection"* by making a *"technical and economical comparison between a 33 kV and 66 kV"*. This topic falls in line with similar research carried out currently, e.g. [40] [49], that challenges the traditional standard wind power plant in order to find more cost effective and technical improved solutions.

The comparison between a 33 kV wind farm and a 66 kV wind farm involved the design and implementation of the wind farms in Digsilent Powerfactory. The comparison and analysis have been based on simulations of different scenarios in Powerfactory focusing on the technical performance of the wind farms in terms of active power losses, reactive power capabilities, fault current and the impact of using wind turbine tap changing transformers. In relation to this, the design of the 33 kV and the 66 kV wind farm and the analysis of their technical performance have been used to estimate and compare relevant economic aspects of the two cases.

Based on the comparison carried out between the two cases in this thesis, it is not possible to conclude that using 66 kV in the collection grid of wind power plants will result in improved technical performance and economic benefits of wind farms. The comparison between the 33 kV and the 66 kV wind farm showed both benefits and disadvantages by using 66 kV compared to 33 kV.

One of the benefits of using 66 kV is lower losses caused by a reduction of the losses in the collection grid cables. However, the decline in losses is small which only leads to a slightly higher annual energy production in the 66 kV wind farm compared to the 33 kV wind farm. The utilisation of the tap changers on the wind turbine transformers also gave a very similar relationship between losses and the tap position in both wind farms. Another benefit of using 66 kV are significantly lower fault current levels in different fault cases compared to using 33 kV, as a results of halving the voltage.

One of the disadvantages that the analysis of the technical performance showed was that in order to fulfil the Danish grid code requirements the reactive power compensation needed in the 66 kV wind farm was slightly higher than the one needed in the 33 kV wind farm. The different reactive power compensation needed also led to a small increase in cost of the shunt reactor used as reactive power compensation in the 66 kV wind farm compared to the one used in the 33 kV wind farm. The added cost of the shunt reactor combined with higher estimated cost of switchgear and wind turbine transformers caused by the higher voltage level resulted in an overall small increase in the installation cost when using a 66 kV rather than 33 kV collection grid. Overall, the economic evaluation based on the investment cost and the annual energy production showed that over the lifetime of the wind farms the cost of energy are about the same for the 33 kV case and the 66 kV case.

The findings in this thesis have been based on only one set up of the wind farms with two different collection grid voltages. Thus, limiting the ability to draw a broader conclusion between the voltage level used in the collection grid and the technical and economical aspects of wind farms. When comparing the work in this thesis with literature of similar investigations, it was also seen that the choice of wind farm layouts and case scenarios to investigate are important factors when determining which voltage level gives better technical performance and economics of wind farms. To decide which voltage level to use therefore depends on the specific wind farm case. Hence, before the results and conclusion of the comparison between the 33 kV and the 66 kV wind farm in this thesis can be used for wind power plant developers in their choice of voltage level in the collection grid, additional studies should be conducted.

In the future, it could be interesting to extend the research in the thesis with more scenarios including different layouts of the wind power plants and more sizes in terms of power or larger/smaller voltage levels. Also other locations of erecting the wind power plants could be interesting to investigate further to include other Weibull distributions of wind speeds and to compare the technical results against grid codes in other countries.

Bibliography

[1] Information obtained through discussion with supervisor Mattia Marinelli.

[2] High voltage cables. `www.elect.mrt.ac.lk/HV_Chap5.pdf`. Accessed: 10-06-2015.

[3] Synchronous generator vs. synchronous motor. `http://educypedia.karadimov.info/library/MG.pdf`. Accessed: 03-06-2015.

[4] *Technical regulation 3.2.5 for wind power plants with a power output greater than 11 kW*. Energinet.dk, 2010.

[5] *ENTSO-E Network Code for Requirements for Grid Connection Applicable to all Generators*. European Network of Transmission System Operators for Electricity, March 2013.

[6] *Implementation Guideline for Network Code "Requirements for Grid Connection Applicable to all Generators"*. European Network of Transmission System Operators for Electricity, October 2013.

[7] *TSO cooperation and the internal energy market*. European Network of Transmission System Operators for Electricity, 2013. ENTSO-E Annual Report 2013.

[8] *World Energy Perspective Cost of Energy Technologies*. World Energy Council, 2013.

[9] *Digsilent Powerfactory 15 User Manual*. Digsilent, May 2014.

[10] Siemens swt-3.6-120 3600 120.0. WindPRO, January 2014. Data provided in DTU course 46200 January 2014.

[11] *66 kV Systems for Offshore Wind Farms*. DNV GL Energy, May 2015. Project name: Tennet, NL Offshore Wind Farm Transmission Systems.

[12] Digsilent powerfactory. `http://www.digsilent.de/`, 2015. Accessed: 03-06-2015.

[13] *The European offshore wind industry - key trends and statistics 2014*. European Wind Energy Association (EWEA), January 2015.

[14] *Offshore wind in Europe Walking the tightrope to success*. Ernst and Young, March 2015.

[15] M J Mulroy A P Neumann and C Ebden. The use of 66 kv technology for offshore wind demonstration sites. (Offshore Renewable Energy Catapult.

[16] ABB. A higher calling. `http://www.abb.dk/cawp/seitp202/1ce06cc33168d0fd44257bdb003afc2e.aspx`. Accessed: 03-06-2015.

[17] ABB. Xlpe submarine cable systems, 2010. Technical manual.

[18] Thomas Ackermann, editor. *Wind power in power systems*. John Wiley and Sons Ltd, 2nd edition, 2012. ISBN 978-0-470-97416-2.

[19] U.S. Energy Information Administration. Levelized cost and levelized avoided cost of new generation resources in the annual energy outlook 2014, April 2014.

[20] The Danish Energy Agency. Accelerating green energy towards 2020. Technical report, Ministry of Climate, Energy and Building, March 2012.

[21] A.I.Adejumobi and O. I. Adebisi. Power loss reduction on primary distribution networks using tap-chaning technique. *International Journal of Research and Reviews in Applied Sciences*, February 2012.

[22] Andrew. Energy numbers. `http://energynumbers.info/capacity-factors-at-danish-offshore-wind-farms`. Accessed: 08-05-2015.

[23] European Wind Energy Association. Offshore wind. `http://www.ewea.org/policy-issues/offshore/`. Accessed: 02-06-2015.

[24] European Wind Energy Association. Offshore wind. `http://www.ewea.org/policy-issues/offshore/`. Accessed: 02-06-2015.

[25] Himanshu J. Bahirat. Comparison of wind farm topologies for offshore applications. *Power and Energy Society General Meeting, 2012 IEEE*, pages 1–9, 2012.

[26] Lea Bigom. Wind. `http://www.kebmin.dk/en/climate-energy-and-building-policy/denmark/energy-supply-and-efficiency/renewable-energy/wind`, December 2014. Accessed: 03-06-2015.

[27] Jerry R. Borland. Tap changers: To tap or not to tap? ecmweb.com/content/tap-changers-tap-or-not-tap, January 1999. Technical Article. Accessed: 03-06-2015.

[28] David Carr. Carbon trust launches 66 kv cable competition. http://www.windpoweroffshore.com/article/1189328/carbon-trust-launches-66kv-cable-competition, May 2013. Accessed: 03-06-2015.

[29] European Commission. The 2020 climate and energy package. http://ec.europa.eu/clima/policies/package/index_en.htm. Accessed: 02-06-2015.

[30] European Commission. 2030 framework for climate and energy policies. http://ec.europa.eu/clima/policies/2030/index_en.htm. Accessed: 02-06-2015.

[31] European Commission. Europe 2020 targets. http://ec.europa.eu/europe2020/targets/eu-targets/index_en.htm. Accessed: 02-06-2015.

[32] Giorgio Corbetta. *Wind in power 2014 European statistics*. European Wind Energy Association (EWEA), February 2015.

[33] Global Wind Energy Council. Global offshore: Current status and future prospects. http://www.gwec.net/global-offshore-current-status-future-prospects/. Accessed: 02-06-2015.

[34] Tom Cronin. Grid connection, January 2014. Lecture notes in DTU course 46200 January 2014.

[35] Edvard Csanyi. Using tap changers to match the system voltage. http://electrical-engineering-portal.com/using-tap-changers-to-match-the-system-voltage, August 2012. Technical Article. Accessed: 03-06-2015.

[36] Edvard Csanyi. An example of transformer tap-changer correct adjustment. http://electrical-engineering-portal.com/example-of-transformer-tap-changer-correct-adjustment, June 2014. Technical Article. Accessed: 03-06-2015.

[37] Edvard Csanyi. 4 essential features of transformer on-load tap changer (oltc). http://electrical-engineering-portal.com/4-essential-features-of-transformer-on-load-tap-changer-oltc, January 2015. Technical Article. Accessed: 03-06-2015.

[38] Dieter Dohnal. *On-load tap changers for power transformers*. Maschinenfabrik Reinhausen, September 2013.

[39] Schneider Electric. 7. reactive energy compensation. Industrial electrical network design guide.

[40] Anna Ferguson et.al. Benefits in moving the inter-array voltage from 33 kv to 66 kv ac for large offshore wind farms. In *International Conference 66 kV for Offshore Wind*, November 2014.

[41] Hamzah Eteruddin and Abdullah Asuhaimi bin Mohd Zin. Reduced dielectric losses for underground cable distribution systems. *International Journal of Applied Power Engineering (IJAPE)*, 1(1):37–46, April 2012.

[42] Jon Jensen Fagertun. Reactive power capability, swt-3.6 vs 50 hz. Siemens Wind Power, 2013. Provided by Siemens Wind Power.

[43] Renewable Energy Focus. Solar and wind dominate world market. `http://www.renewableenergyfocus.com/view/33730/solar-and-wind-dominate-world-market/`, July 2013. Accessed: 02-06-2015.

[44] Sven-Erik Gryning et al. Long-term profiles of wind and weibull distribution parameters up to 600 m in a rural coastal and an inland suburban area. *Boundary-Layer Meteorology*, 150:167–184, February 2014.

[45] Anca D. Hansen. Introduction to wind power models for frequency control studies, September 2013. Compendium from DTU course 46230 Autumn 2013.

[46] Kurt Hansen and Anders Sommer. Wind resources at horns rev. Technical report, Tech-wise A/S, December 2002.

[47] Wind Measurement International. Operational and maintenance costs for wind turbines. `http://www.windmeasurementinternational.com/wind-turbines/om-turbines.php`. Accessed: 03-06-2015.

[48] Thomas J. Overbye J. Duncan Glover, Mulukutla S. Sarma. *Power System Analysis and Design*. Global Engineering, 5th edition, 2012.

[49] Henrik Kirkeby and John Olav Tande. The nowitech reference wind farm. In *EERA DeepWind'2014 Deep Sea Offshore Wind R and D Conference*, 2014.

[50] P. Kundur. *Power System Stability and Control*. McGraw-Hill, 1994.

[51] J. Rohan Lucas. Power system fault analysis, October 2005. Lecture notes produced by The University of Moratuwa, Department of Electrical Engineering.

[52] Stefan Lundberg. Performance comparison of wind park con

gurations. Technical report, Department of Electric Power Engineering, School of Electrical Engineering, Chalmers University of Technology, Goteborg, Sweden, 2003.

[53] M. Pisani M. Trovato M. Dicorato, G. Forte. Guidelines for assessment of investment cost for offshore wind generation. *Renewable Energy*, 36:2043–2051, 2011.

[54] Mattia Marinelli. Power systems stability and control – an overview, October 2014. Power point presentation from DTU course 31783 autumn 2014.

[55] Cesar Augusto Quintero Marron. *Challenges of the integration of wind park clusters into power grids*. Books on Demand, 2014. ISBN: 9783732298761.

[56] Megavind. The danish wind power hub, strategy for research, development, and demonstration. Technical report, Magavind, May 2013.

[57] Meteotest. The swiss wind power data website. `http://wind-data.ch/tools/weibull.php?lng=en`. Accessed: 08-05-2015.

[58] G.F. Moore. *Electric Cables Handbook*. Blackwell Science Ltd., 3rd edition, 1997.

[59] Niels G. Mortensen. Wind resource assessment using the wasp software. DTU Wind Energy, December 2014. Course notes for DTU course 46200 January 2014.

[60] Poul-Erik Morthorst and Shimon Awerbuch. *The Economics of Wind Energy*. European Wind Energy Association, March 2009.

[61] nkt cables. *Teknisk katalog 2013*, 2013. Technical manual.

[62] National Programme on Technology Enhanced Learning. Fault analysis. `http://nptel.ac.in/courses/108107028/module4/lecture6/lecture6.pdf`. Accessed: 03-06-2015.

[63] Sonal Patel. Iea: Wind power could supply 18`http://www.powermag.com/iea-wind-power-could-supply-18-of-worlds-power-by-2050/`, January 2013. Power Magazine. Accessed: 03-06-2015.

[64] Colin Pawsey. The race to develop cables for 66 kv. In *International Conference 66 kV for Offshore Wind*, November 2014.

[65] Garrad Hassan Ronan Mc Dermott and Partners Ltd. Investigation of use of higher ac voltages on offshore wind farms. EWEC, 2009.

[66] J. Declercq R.V. Schevensteen, Y. Vanlinthout. The life starts at 36 project: development of wind turbine generator transformers above 36 kv. In *CG Power Systems*. EWEA, 2013.

[67] M. Hand B. Maples A. Smith S. Tegen, E. Lantz and P. Schwabe. 2011 cost of wind energy review. Technical report, National Renewable Energy Laboratory, March 2013.

[68] D. Saez et al. Evaluation of 72 kv collection grid on offshore wind farms. In *EWEA Annual Event*, Copenhagen, April 2012.

[69] IRENA Secretariat. *Renewable Energy Technologies: Cost Analysis Series, Wind Power*, volume 1. IRENA, 2012.

[70] Nord Pool Spot. Elspot prices. `www.nordpoolspot.com/Market-data1/Elspot/Area-Prices/ALL1/Yearly/?view=table`, 2014. Accessed: 03-06-2015.

[71] S. Tegen, M. Hand E. Lantz, B. Maples, A. Smith, and P. Schwabe. 2011 cost of wind energy review. Technical report, National Renewable Energy Laboratory, March 2013.

[72] Nasser D. Tleis. *Power Systems Modelling and Fault Analysis*. Elsevier Ltd., 2008. ISBN-13: 978-0-7506-8074-5.

[73] Vestas. Life cycle assessment of offshore and onshore sited wind power plants based on vestas v90-3.0 mw turbines. Technical report, Vestas Wind Systems A/S, Randers, Denmark, 2006.

[74] Renewable Energy World. Why is renewable energy important? `http://www.renewableenergyworld.com/index/tech/why-renewable-energy.html`. Accessed: 02-06-2015.

Appendix

A.1 ABB Datasheet Submarine Cable Systems

Cross section mm²	Copper conductor	Aluminium conductor
	A	A
95	300	235
120	340	265
150	375	300
185	420	335
240	480	385
300	530	430
400	590	485
500	655	540
630	715	600
800	775	660
1000	825	720

Figure A.1: Current rating for three-core submarine ABB cables [17].

Cross-section of conductor	Diameter of conductor	Insulation thickness	Diameter over insulation	Lead sheath thickness	Outer diameter of cable	Cable weight (Aluminium)	Cable weight (Copper)	Capacitance	Charging current per phase at 50 Hz	Inductance
mm²	mm	mm	mm	mm	mm	kg/m	kg/m	µF/km	A/km	mH/km
Three-core cables, nominal voltage 66 kV (Um = 72.5 kV)										
95	11.2	9.0	31.6	1.3	113.0	19.8	21.6	0.17	2.0	0.44
120	12.6	9.0	33.0	1.4	116.0	21.6	23.8	0.18	2.1	0.43
150	14.2	9.0	34.6	1.4	120.0	22.9	25.7	0.19	2.3	0.41
185	15.8	9.0	36.2	1.4	124.0	24.5	28.0	0.20	2.4	0.40
240	18.1	9.0	38.5	1.6	129.0	26.8	31.3	0.22	2.6	0.38
300	20.4	9.0	40.8	1.6	134.0	28.7	34.3	0.24	2.8	0.37
400	23.2	9.0	43.6	1.7	141.0	31.7	39.2	0.26	3.1	0.35
500	26.2	9.0	47.0	1.9	149.0	36.0	45.4	0.29	3.5	0.34
630	29.8	9.0	50.6	2.0	157.0	40.1	52.0	0.32	3.7	0.33
800	33.7	9.0	54.5	2.1	167.0	45.1	60.1	0.35	4.1	0.32
1000	37.9	9.0	59.3	2.3	178.0	51.8	70.7	0.38	4.6	0.31

Figure A.2: Technical data for ABB 66 kV three-core submarine cables [17].

A.2 Cost Expression Parameters

The cost expressions presented in 5.5 are based on [52]. The parameters used in the cost expressions are captured in A.1. Note that the cost expression from [52] originally are calculated in Swedish Kroner, hence, the results have been converted in to Euro as presented in the economic analysis of the two wind farms.

	Parameter	**Value**
Cable Cost Parameters		
	$A_{cable\,33kV}$	$0.411*10^6$
	$B_{cable\,33kV}$	$0.596*10^6$
	$C_{cable\,33kV}$	$4.1/10^8$
	$A_{cable\,66kV}$	$0.688*10^6$
	$B_{cable\,66kV}$	$0.625*10^6$
	$C_{cable\,66kV}$	$2.05/10^8$
	$A_{cable\,132kV}$	$1{,}971*10^6$
	$B_{cable\,132kV}$	$0.209*10^6$
	$C_{cable\,132kV}$	$1.66/10^8$
Transformer Cost Parameters		
	A_{trf}	$-1.208*10^6$
	B_{trf}	2143
	β_{trf}	0.4473
Switchgear Cost Parameters		
	A_{SG}	$320*10^3$
	B_{SG}	6

Table A.1: Parameters of the cost expression used to estimate the cost of components in the 33 kV wind farm and 66 kV wind farm [52].